Archives of Computational Methods in Engineering (2020) 27:455–478
https://doi.org/10.1007/s11831-019-09329-9

ORIGINAL PAPER

State-of-the-Art Review of Metallic Dampers: Testing, Development and Implementation

Ahad Javanmardi[1] · Zainah Ibrahim[1] · Khaled Ghaedi[1] · Hamed Benisi Ghadim[2] · Muhammad Usman Hanif[3]

Received: 1 January 2018 / Accepted: 21 February 2019 / Published online: 1 March 2019

Abstract
Structural control systems have gained popularity for the ability to reduce the structural vibration response of civil structures subjected to different types of dynamic loads. Passive, semi-active, active and hybrid control systems have been widely utilized in various types of structures. This article presents one of the most economical and yet the most effective approaches used in structural vibration control. Herein, a comprehensive state-of-the-art review of the development and application of metallic dampers is discussed. The dampers are classified into five categories: steel, aluminum, lead, copper and shaped-memory alloy dampers. In addition, the details of various computational methods used in the analysis of metallic dampers are briefly explained. This article reveals that the use of metallic dampers is being advanced broadly owing to their low manufacturing costs, stable hysteresis behavior, resistance to ambient temperature, reliability and high energy dissipation capability. It is also concluded that mild steel is the most popular material among metallic dampers.

1 Introduction

Civil structures are commonly subjected to various types of dynamic and environment loadings, such as wind, traffic and earthquakes. In particular, earthquake events cause severe damage to building and bridge structures. For instance, during the Mexico City earthquake in 1985, more than 132 buildings collapsed or were heavily damaged. In 1989, Northern California was shaken by the Loma Prieta earthquake when over 200 buildings suffered severe damages [1]. To prevent or mitigate such damage, structural vibration controls have been developed greatly and utilized skillfully in different civil structure locations. Structural vibration control systems are generally divided into four major categories: passive, active, semi-active and hybrid systems [2, 3] and several state-of-the-art review articles briefly discuss these categories [2–13]. Control systems can be used in the seismic hazard mitigation of new structures as well as in the retrofitting of aged structures with low lateral strength such as precast frames [14–20]. Among all categories, passive systems are one of the most popular structural vibration controls [21–26] as they are inexpensive and protect structures against seismic loads without any source of external energy and control algorithm during operation. The main characteristic of passive control systems is that they provide additional damping and/or stiffness to the structure without any external energy source. Such systems are commonly divided into seismic isolation systems and energy dissipation devices (dampers). In the past few decades, various seismic isolation systems have been developed and implemented in large-scale civil structures with high logistic value [27–30]. In addition, passive energy dissipation devices are categorized as hysteresis devices, viscoelastic devices, tuned mass dampers, magnetic negative stiffness devices, resetting passive stiffness devices and viscous dampers [31]. Furthermore, hysteresis devices are divided into metallic and friction dampers, whose energy dissipation is independent of loading rate. Metallic dampers dissipate energy through the inelastic deformation of their constitutive material. The advantages of metallic dampers over active and semi-active dampers are stable hysteretic behavior, rate independence, resistance against ambient temperature and reliability, and the fact that practice engineers are familiar with their material behavior.

✉ Ahad Javanmardi
Ahadjavanmardi@gmail.com; Ahad@siswa.um.edu.my

[1] Present Address: Civil Engineering Department, University of Malaya, 50603 Kuala Lumpur, Malaysia

[2] Department of Water Resources Management and Harbor Engineering, Fuzhou University, Fuzhou, Fujian, China

[3] School of Civil and Environmental Engineering (SCEE), National University of Sciences and Technology, H-12, Islamabad, Pakistan

As mentioned in the literature, a number of researchers have reported the usefulness of passive devices. It is also concluded that amongst several types of passive dampers, the metallic dampers have so far attracted a lot of attention from civil engineers. Despite the lack of updated studies that present and advance informative reviews of metallic control systems, Skinner et al. [32], Kobori et al. [33] and Nakashima et al. [34] highlighted the advancements of metallic dampers. Hence, this paper provides a comprehensive state-of-art review of the development and implementation of metallic dampers in structural vibration control systems since the 1970s.

2 Testing Procedure of Metallic Damper

In order to evaluate the performance of metallic dampers, two tests may be performed: (i) the quasi-static cyclic test and (ii) the shaking table test. The quasi-static test can be conducted on the dissipation device itself or on the structure equipped with energy dissipation devices. According to FEMA 461 [35], the quasi-static cyclic test is a standard procedure to determine the capacity of the energy dissipating device on which deformation is imposed. In the quasi-static cyclic test, loading can be in the form of shear, bending or torsion, whereby the loading protocol is a displacement control that consists of several incremental or constant amplitudes of cycle displacements. Because metallic dampers are rate-independent, the loading rate is not an important factor during the test. For the shaking table test, the damper must be assembled on the scaled or full-scale structure depending on the shaking table dimensions. Artificial or actual ground motion records are used as input loading in the test. Detailed information about both tests is given in FEMA 461 [35]. Metallic damper performance evaluation is based on the force–displacement hysteresis loops obtained from the mentioned tests. Ultimately, the mechanical factors listed in Table 1 can be obtained and calculated from the hysteresis loops of the metallic dampers.

Table 1 Mechanical parameters of metallic dampers

Parameters	Symbol
Yield displacement	Δ_y
Ultimate displacement	Δ_u
Yield strength	P_y
Ultimate strength	P_u
Ductility	μ
Cumulative ductility	μ_{cum}
Effective stiffness	K_{eff}
Total dissipated energy	E_d
Cumulative displacement	Δ_{cum}
Equivalent viscous damping	ξ

3 Hysteresis Behavior of Metallic Dampers

Since metal materials have nonlinear behavior, the hysteretic behavior of metallic materials is advantageous in dissipating dynamic energy, especially in linear systems. This section briefly describes how metal materials behave under cyclic loadings. The metallic material under static loading is plasticized when the stress level exceeds the elastic limit (σ_y) and thereafter enters the stress hardening phase if subjected to larger stresses. Under cyclic loadings, the elastic modulus (E) of the material recovers as the material unloads. If a load is applied in the opposite direction, the material begins to yield and soften at a lower stress level than the yield stress, which is known as the Bauschinger effect [36]. The hysteretic behavior of the material continues as long as the strain does not exceed the yield plateau and the maximum positive and negative stresses remain within the yield stress ($\pm\sigma_y$). The material follows the initial elastic stiffness even after unloading from the stresses higher than the yield plateau. The Bauschinger effect becomes more dramatic as the material reaches toward maximum strain. The metal material promotes a certain post-yield stiffness and the yield plateau disappears during this range of cyclic loading. General schematic hysteresis loops of metallic materials are shown in Fig. 1a [37]. However, the hysteretic behavior may slightly differ depending on the geometry of the metallic dampers. The hysteresis trends of metals, such as steel, aluminum, lead and copper are similar. The stress–strain relationship of steel material is often simplified as a bilinear or trilinear elastoplastic model. The shape memory alloy (SMA) hysteretic behavior is slightly different from other metal materials. The hysteresis loops of SMA are shown in Fig. 1b. SMA exhibits two different behaviors based on the material temperature relative to its austenitic finish temperature, A_f [38]. As the temperature rises above A_f, the strains obtained during loading recover after unloading. During this process, a significant amount of energy dissipates without any sign of residual strains, which is called super-elasticity. The residual strains remain after unloading if the material temperature is below A_f and thereafter the residual strains recover if the material reheats again. This effect is known as the shape memory effect.

4 Classification of Metallic Dampers

The damping mechanism and performance of metallic dampers are greatly dependent on the constitutive material, such as steel, aluminum, copper, etc. Therefore,

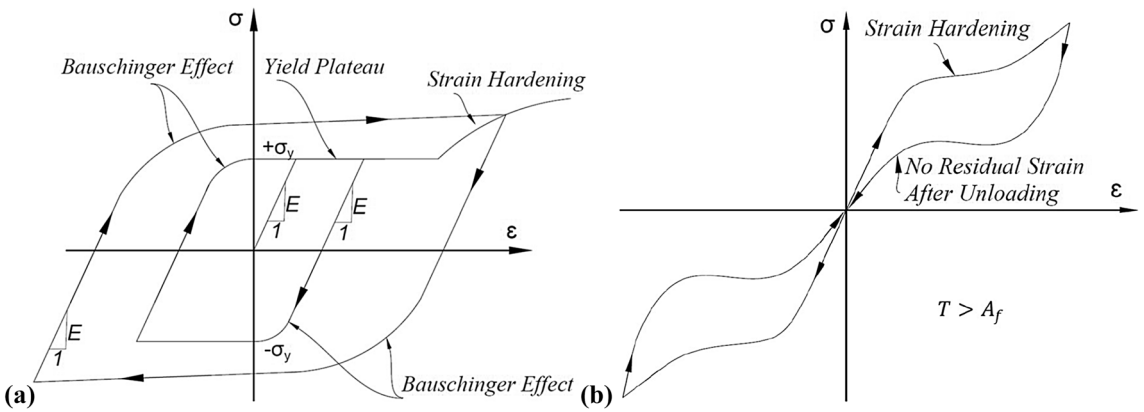

Fig. 1 Idealized hysteresis behavior of **a** metallic and **b** SMA materials

metallic dampers are classified according to their constitutive material into the following categories.

4.1 Steel Dampers

The very first steel dampers were proposed by Kelly et al. in the early 1970s [39]. Thereafter, the U-strip damper, torsional beam damper, flexural beam damper and single-axis damper were developed and tested for implementation in structures as shown in Fig. 2a–d [32]. The U-strip damper consists of a U-shape steel strip placed between the moving plates (Fig. 2a). The U-strip damper is deformed in one direction, thus exhibiting large deformation in the elastic range. The torsional beam damper is made of a square or rectangular plate with fixed ends, whereby the middle segment is subjected to the predominating torsional and flexural movements (Fig. 2b). The torsional beam damper has high load-bearing capacity and may be implemented at the base of structures to prevent structural uplifting caused by severe earthquakes. In contrast, the flexural beam damper is slightly more complex. The main part of the damper is a square or circular section anchored at the bottom and top, allowing rotation and displacement (Fig. 2c). This damper is robust and dissipates seismic loads bidirectionally. The single-axis beam damper is made of a wide beam with high loading capacity (Fig. 2d). Two or more beams may be used together to form a compact damper, which is suitable for the diagonal element of flexible frame structures.

The tapered-steel energy dissipation device was suggested by Tyler [40]. This device is comprised of a taper-shaped round steel bar or steel plate welded to the anchorage plate at the base to form a cantilever (Fig. 2e). The device dissipates energy, taking advantage of the steel material's

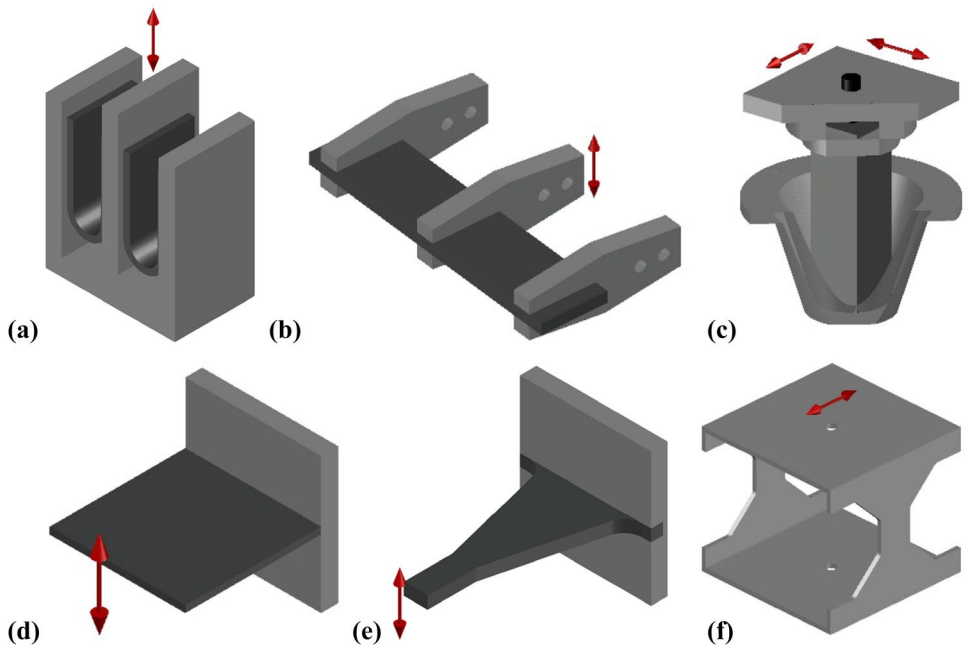

Fig. 2 **a** U-Shaped steel, **b** torsional beam, **c** flexural beam, **d** single-axis, **e** tapered cantilever and **f** taper tube dampers. The loading directions are indicated by arrows

plastic deformation. Pinelli et al. [41] proposed a different type of steel damper based on a steel tube. The proposed device is made of a rectangular steel tube cut into a taper shape at two sides, such that the stresses distribute uniformly along the tapered section of the tube (Fig. 2f).

The buckling-restrained brace (BRB) is another type of steel damper that was initially introduced by Takeda et al. in 1976 [42]. As shown in Fig. 3a, the BRB entails conventional bracing (as the core) encased with a square hollow steel section filled with mortar material. The steel core sustains axial loads while the infilled material eliminates the shear transfer under compression loading to the outer tube. The BRB was further developed with different core configurations, like circular core (CBRB), cross and crosswise core and linear core (Fig. 3c) [43, 44]. These have been implemented extensively worldwide, especially in Japan and the United States since 1987 [45]. For instance, Black et al. [44] conducted comprehensive testing on BRB and concluded that the BRB is a more reliable and practical alternative than conventional bracing systems. Due to the key concerns with BRBs such as inconsistent material behavior, low-cycle fatigue life and steel core geometric imperfections, Zhao et al. [46] introduced another BRB device called the angle buckling-restrained brace (ABRB), as depicted in Fig. 3b. The ABRB consists of four angled steel plates welded together at the ends with stiffeners and connectors. Two other angle plates are welded together around the four angle plates to form a square tube. ABRB failure has been observed at the welded ends of the angle plates. Furthermore, it was designed such that the steel core would remain in the elastic range during rapid loadings. Hao et al. [47] developed the H-type steel unbuckling brace (SUB) consisting of a steel plate core confided in steel element. The end of the steel core plate is connected to Phillips shaped steel plates as shown in Fig. 3d. The confiding element prevents steel core buckling under compression and tension loadings. The SUB damper controls structural displacement by adding stiffness to the frame system. Recently, Dongbin et al. [48] proposed a new type of BRB damper with a circular core configuration (CBRB). The damper is composed of three circular steel tubes, where the core tube with slotted holes is restrained by the inner and outer tubes against any out-of-plane buckling deformation. The restrained tubes are spot welded in the middle to the core tube. CBRB is relatively lighter than existing conventional BRBs.

A very famous metallic damper, the added damping and stiffness (ADAS) device, was proposed by Bergman [49]. ADAS consists of X-shaped steel plates connected in parallel to the base plate using bolts that add extra damping and stiffness to the structure (Fig. 4a). Afterwards, Tsai et al. [50] developed the triangular-plate added damping and stiffness (TADAS) device based on the ADAS concept. The TADAS mechanism is similar to ADAS, whereby several triangular steel shaped plates are welded in parallel to the base plate and the narrow end is locked to another plate with bolts (Fig. 4b). Both ADAS and TADAS dampers are suggested for moment resistant frames to increase the damping and stiffness of the structures. Shih et al. [51, 52] developed a rhombic ADAS damper using low yield strength steel with hinge supports at both ends (Fig. 4c). The hinge supports eliminate unfavorable axial forces on the plate. The strain hardening quality of low yield strength steel helps control the problem of local fractures in the damper. In addition, the mechanical properties of low yield strength steel reduce the yield displacement and enhance the energy dissipation capability and ductility of the damper [53]. Damper symmetry also reduces the effects of welding on the performance of the damper.

Li and Li [54] introduced the dual function damper with three different geometries: single round-hole, X-shaped and

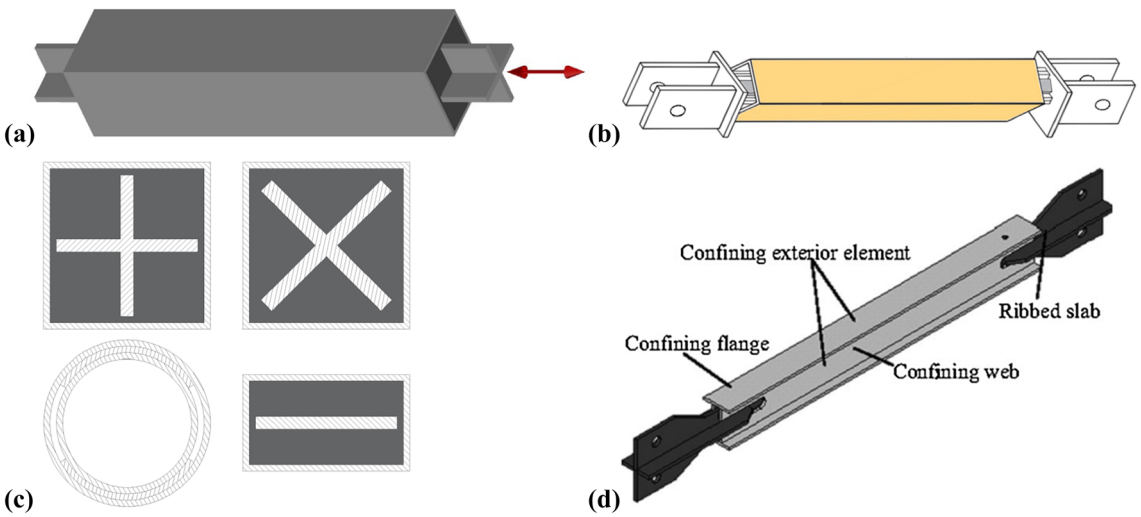

Fig. 3 Schematic views of **a** BRB, **b** ARBRB [45], **c** different BRB core configurations and **d** SUB [46]

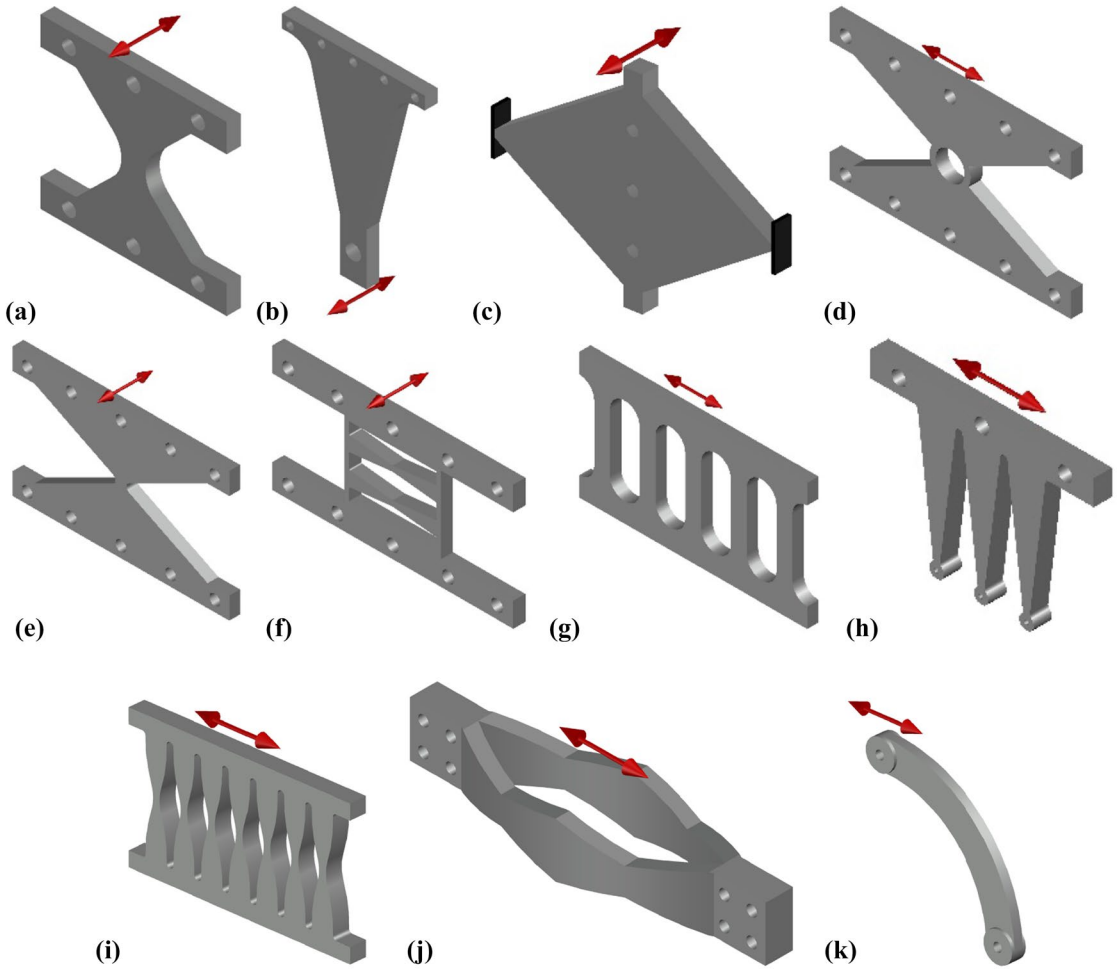

Fig. 4 Steel plate-based dampers, **a** ADAS, **b** TADAS, **c** rhombic, **d** single round-hole, **e** X-shaped, **f** double X-shaped, **g** slit, **h** comb-teeth, **i** parabolic, **j** pre-bent strips and **k** curved steel dampers

double X-shaped metallic dampers as illustrated in Fig. 4d–f. Dual function dampers are a type of ADAS devices. The single round-hole metallic damper is made of a hollow circular cross-section in the middle of an X-shaped steel plate, whereas the X-plate damper has a narrower section in the middle of the X-plate. The dual X-shaped damper consists of two Xs placed in series. The load is applied parallel to the round-hole damper and perpendicular to X-shaped and double X-shaped dampers. The slit steel damper (SSD) was invented by Chan and Albermani [55] and was subsequently developed by several others researchers [56–59]. The SSD is made of a standard structural wide-flange section with several slits cut in the web section as shown in Fig. 4g. The slits are rounded at the ends to prevent stress concertation during seismic events. The device can be connected to the primary structure using bolts, therefore preventing uncertainties associated with welding. The first suggested installation of the SSD was in an inverted V-brace system. Oh et al. [60] tested the SSD performance at the beam-column connection of steel structures and found significant enhancement in the seismic performance of the connection.

Garivani et al. [61] introduced the comb-teeth damper (CTD) for using in chevron bracing systems. As Fig. 4h illustrates, the CTD is made of a steel plate cut in the shape of comb teeth. The top and bottom parts of the CTD damper are connected to a frame with bolts. A CTD subjected to in-plane flexural deformation dissipates energy through the yielding of the comb teeth. The CTD has shown out-of-plane behavior during experimental tests, which was eliminated by enlarging the CTD plate thickness. Fan et al. [62] took advantage of low yield strength steel and developed a new two-stage energy dissipation device, as depicted in Fig. 4i. The device is composed of several parabola openings in the steel plate. The plate is welded to the top and bottom anchorage plates. The device dissipates energy through shear deformation of the plate inflection points. Wang and Chien [63] presented a device based on bent steel strips, as shown in Fig. 4j. The device consists of two pre-bent

steel strips bolted to connectors. The device is loaded axially and the strips are subjected to buckling deformation. The force–displacement hysteresis loops of a pre-bent steel strip damper found to be asymmetric. Nonetheless, symmetric hysteresis behavior is achieved when pre-bent steel strip dampers are coupled. Hsu and Halim [64] proposed a steel curved damper for moment-resisting frames. The damper has a curve shape and is made from steel plates (Fig. 4k). The damper's performance was tested in a beam-to-column connection. The lateral movement generated eccentricity to the curved damper, thereby increasing the lateral stiffness of the beam-column connection.

Nakashima et al. [65] proposed the shear panel damper (SPD), which contains a steel plate welded to the top and bottom plates (Fig. 5a). The SPD has large energy dissipation capability. Abebe et al. [66] pointed out the failure modes of the SPD, i.e. failure at the shear panel center, failure at the shear panel corners and flange weld failure. Chen et al. [67, 68] enhanced the SPD performance by adding stiffeners. The stiffened shear panel damper (SSPD) illustrated in Fig. 5b is made of a shear panel with horizontal and vertical stiffeners. The stiffness of SSPD is relatively higher than conventional SPDs, as it promotes large deformation with no signs of pinching and strength degradation. Subsequently, Zhang et al. [69] improved the SPD performance using low yield strength steel. In addition, the shape optimization method was used to optimize the damper's dissipation performance [70]. Chan et al. [71] proposed the yielding shear panel device (YSPD). This device is made of a thin steel plate welded inside a short segment of square hollow steel (Fig. 5c). YSPD is subjected to in-plane loading and the steel plate undergoes shear deformation to harvest the induced energy. Moreover, Chan et al. [72] proposed another damper called the perforated yielding shear panel device (PYSPD). This is a modified version of YSPD as a thin steel plate has a number of circular holes. The undesirable local deformation in the YSPD corners can be eliminated by perforating the steel plate in PYSPD.

Sahoo et al. [73] used a combination of the X-plate damper and SPD to innovate a new energy dissipating device known as the shear-and-flexural yielding damper (SAFYD). This damper consists of a shear steel plate at the center and two X-shaped steel plates on both ends, as illustrated in Fig. 5d. The damper energy dissipation mechanism is a combination of the flexural deformation of the X-plates and the shear deformation of the web plate. Consequently, great lateral strength and stiffness are exhibited in SAFYD. Deng et al. [74] proposed another type of SPD, namely the buckling restrained shear panel damper (BRSPD), which is made of a steel shear panel restrained by two plates (Fig. 5e). The restrained plates sandwich the shear panels by means of bolts to reduce out-of-plane buckling deformation of the shear panels.

The J-damper, made of four J-shaped plates and arranged as shown in Fig. 6a, was invited by Kato et al. [75]. All J-shaped plates are bolted to a plate in the middle with roller supports at the pate's end. The damper dissipation mechanism is based on the roll-bending movement of the steel plates that work effectively under large deformation due to the plates' shape. Deng et al. [76] developed the crawler steel damper that benefits from U-shaped steel plates. The damper contains two U-shaped steel plates facing each other and clamped between two connection plates. The plate arrangement, as illustrated in Fig. 6b, prevents stress concentration

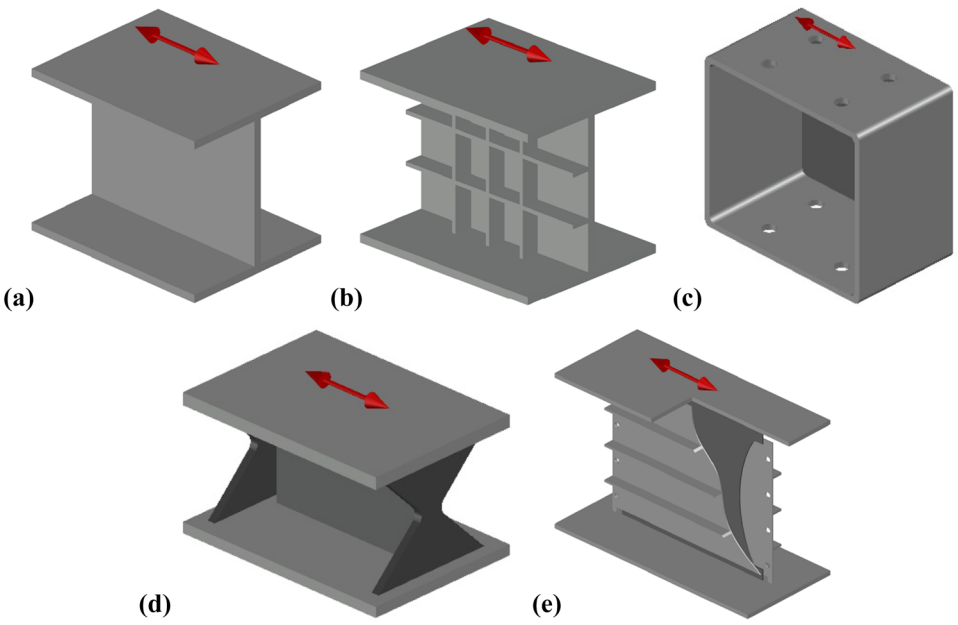

Fig. 5 Steel shear panel-based dampers. **a** SPD, **b** SSPD, **c** YSPD, **d** SAFYD and **e** BRSPD

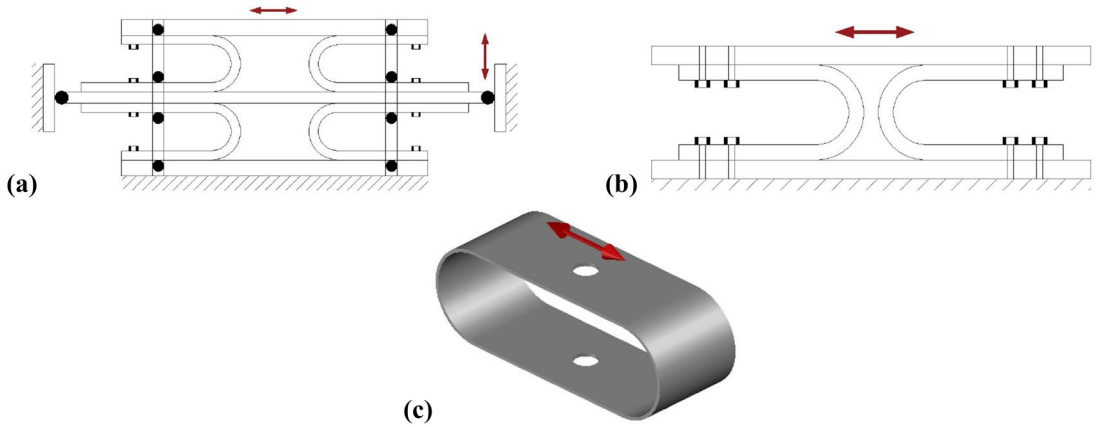

Fig. 6 Detailing of **a** J-damper, **b** crawler damper and **c** cushion damper

in one plate, hence substantially improving the damper performance during low-cycle fatigue loadings. Subsequently, the damper's dissipation capacity is mostly dominated by the U-shaped plates' height and thickness. The steel cushion was introduced as an energy harvesting device in chevron bracing systems [77]. As Fig. 6c demonstrates, the cushion is a cushion-shaped steel plate bolted to the primary structure. The device undergoes in-plane shear deformation to dissipate energy and has a high displacement capacity under low to moderate earthquake loads.

The tube-in-tube damper (TITD) was invented by Benavent-Climent [78]. The concept of TITD is inspired by BRB and SSD and was proposed for bracing systems. The TITD consists of two concentric rectangular hollow sections inserted into each other. The outer tube had several slit cuts. As Fig. 7a demonstrates, the two tubes are welded to a plug and fillet. The damper is loaded axially at the ends of the two tubes, while the slit strips dissipate the load through plastic deformation. Furthermore, Benavent-Climent et al. [79] took advantage of the structural I-beam or wide flange to reduce the welding uncertainties in metallic dampers to develop another energy dissipation device. The device comprises several short segments of I-beams placed in parallel and bolted to two auxiliary elements (Fig. 7b). The auxiliary elements are subjected to axial loads in the brace system, while the web of I-beams is subjected to out-of-plane bending.

The pipe damper (PD) is made of a short structural steel pipe segment placed horizontally and welded to bottom and top plates. The PD was presented by Maleki and Bagheri [80] and is shown in Fig. 8a. In addition, Maleki and Mahjoubi [81] also investigated the behavior of a dual-pipe damper (DPD). The DPD mechanism is similar to PD, with two pipes welded to each other (Fig. 8b). The DPD demonstrates higher energy dissipation capacity than the PD. Thereafter, Maleki and Mahjoubi [82] used different infills to enhance the energy dissipation capability of the PDP. Similarly, the infilled-pipe damper (IPD) has two pipe sections welded to two smaller diameter concentric pipes. The gap between the two concentric pipes is filled with lead or zinc materials, as presented in Fig. 8c. Two cover plates are bolted at the sides of the pipes to prevent the squeezing out of the infill materials during operation. The plastic deformation of the inner and outer steel pipes as well as the infill materials is the main IPD feature to mitigate the shear stresses caused by lateral forces. Consequently, the IPD performance is significantly better than the PD and DPD. Franco et al. [83] proposed a torsional tube damper (TTD),

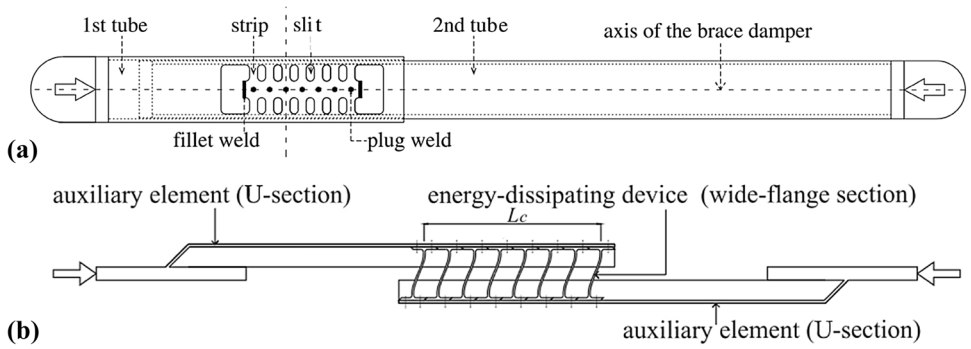

Fig. 7 Detailing of dampers proposed by Benavent-Climent [78, 79]

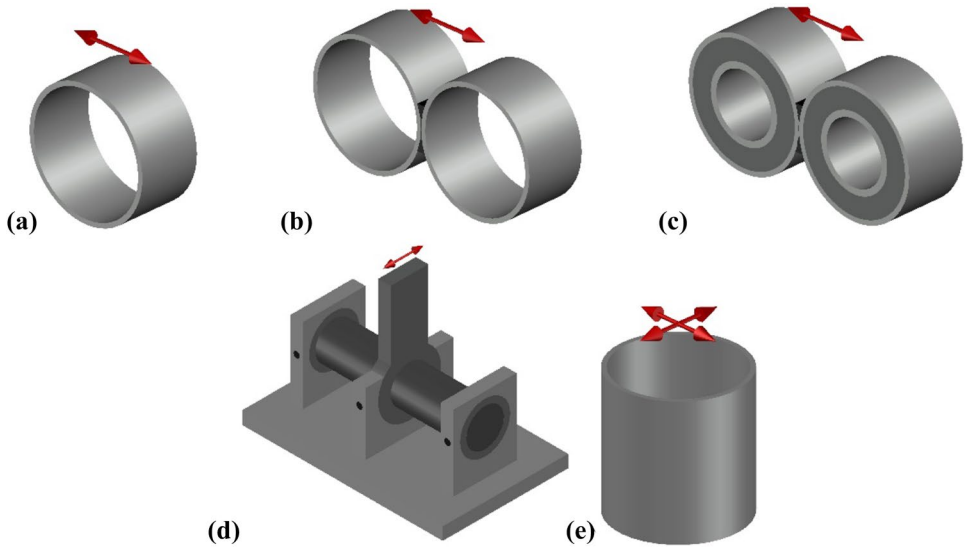

Fig. 8 Schematic view of pipe-based dampers, **a** PD, **b** DPD, **c** IPD, **d** TTD and **e** VPD

which consists of a central tube of low-carbon steel fixed at both ends and connected in the middle to a lever arm. The lever arm is attached to the anchorage supports and rotates in a torsional manner (Fig. 8d). Thereby, the shear and bending loads are eliminated, ultimately leading to high cumulative displacement and energy dissipation. Furthermore, Javanmardi et al. [84] presented a vertical pipe damper (VPD) made of a short vertical pipe segment welded to two anchor plates (Fig. 8e). The VPD is able to dissipate energy bidirectionally and has greater ductility and energy dissipation capability than the PD and DPD.

The elastic–plastic steel damper (EPSD) is made of several E-shaped steel plates with hinged ends and attached with pins to the connecting plate. The EPSD was developed by Wang et al. [85] and is depicted in Fig. 9a. The E-shaped plates can be arranged symmetrically either on both sides or only on one side of the connecting plate. The EPSD dissipates shear force from the connecting plate through the pins to the E-shaped plates. Yamazaki et al. [86] proposed a novel buckling-restrained rippled plate damper (BRRPD) for use in the event of large earthquakes. The BRRPD contains a rippled core plate with two restraining plates on both sides (Fig. 9b). The restraining steel plates are bolted to the rippled core plate and the base plate. The governing factor in BRRPD design is identified as the gap size between the core plate and restraining plates. The device demonstrates two deformation modes: (i) expansion deformation and (ii) out-of-plane global buckling deformation. The BRRPD has exhibited stable hysteretic behavior and high-energy dissipation capacity in different experimental tests.

Ghaedi et al. [87, 88] proposed a new metallic damper called Bar Damper (BD) based on flexural deformation of solid steel bars. As Fig. 9c shows, it is consisted of several solid bars welded to the top and bottom steel plates. The BD showed excessive energy dissipation capability under large deformation with no sign of stiffness and strength degradation. The accordion metallic damper (AMD) was developed based on the mechanism of shock absorbers in the machinery industry [89]. The AMD is fabricated from a thin-wall accordion steel tube, both ends of which are welded to end plates (Fig. 9d). The axial load dissipates by plastic formation in the corrugated tube. The AMD exhibits asymmetric hysteretic behaviour, but the symmetric behaviour is achieved when AMDs are coupled. Aghlara and Tahir [89] invented the bar-fuse damper (FBD), which is made of inner, outer and fuse parts (Fig. 9e). The outer part consists of a square steel tube, while the inner part comprises two C-channels welded to each other with a middle plate. The middle plate and outer part have several holes to accommodate the fuse bars. The steel bars are bolted to the inner and outer parts. The FBD is loaded axially and dissipates energy through the plastic deformation of the steel bars. The key feature of FBD is the easy replacement of the steel bars after failure. Thereafter, Aghlara et al. [90] developed the pipe-fuse damper (PFD) based on the FBD concept. PFD also consists of inner, outer and fuse parts similar to FBD. However, in the fuse part, the steel bars are replaced with steel pipes. PFD also has the same energy dissipation mechanism as FBD, except PFD has higher energy dissipation capability.

4.2 Aluminum Damper

Aluminum offers greater ductility and lower yielding displacement compared to mild steel and low yield strength steel. De Matteis et al. [91, 92] presented an energy dissipating device based on pure aluminum with the same geometry as the YSPD. The shear panel is used in the

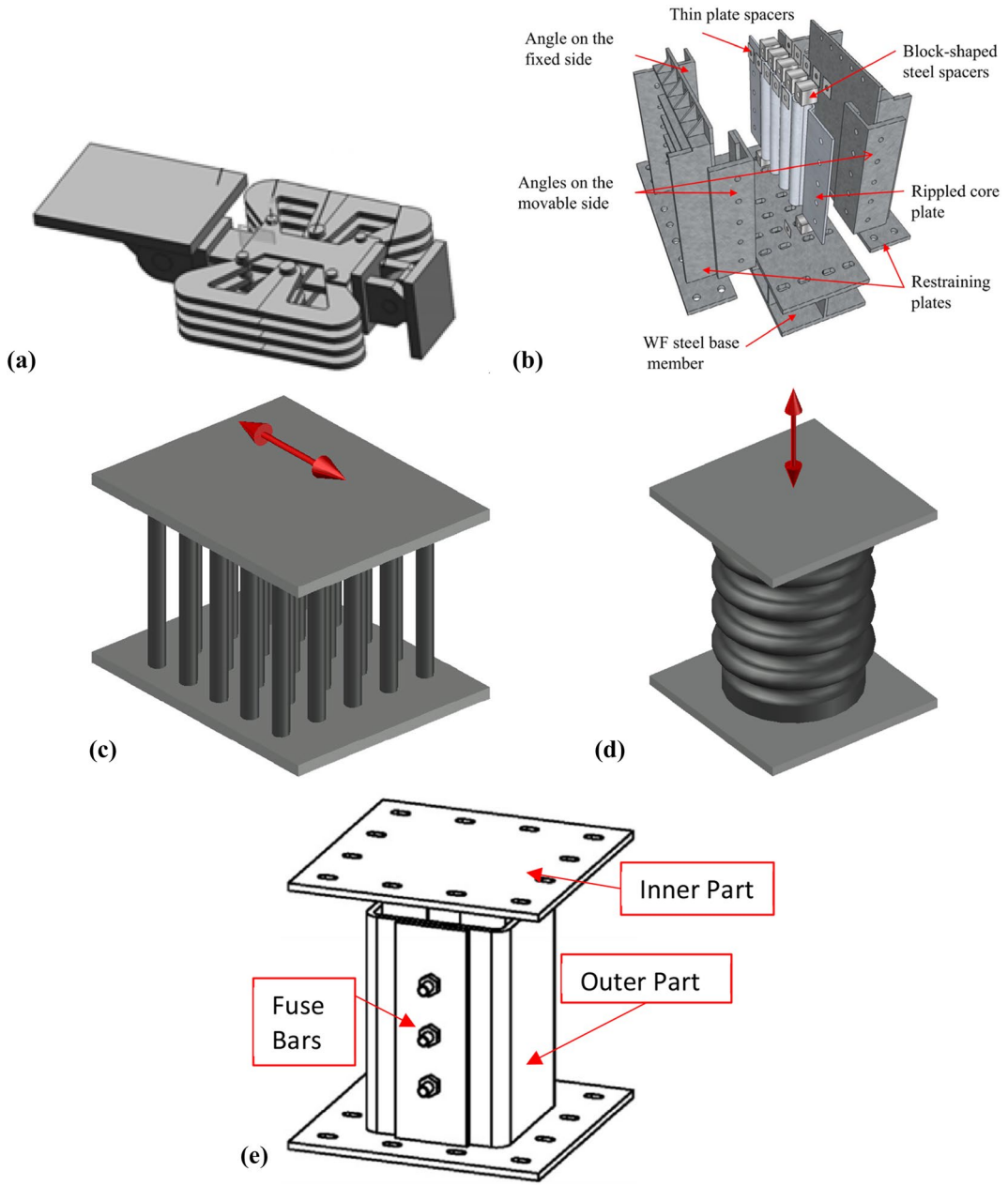

Fig. 9 Detailing of: **a** EPSD [84], **b** BRRPD [85], **c** BD, **d** AMD and **e** FBD [88]

steel moment-resisting frame for lateral stability of the structure. The device is made of thin aluminum plates to form a short H-section segment with stiffeners as shown in Fig. 10. The damper's performance was tested in a frame system through the shaking table test and it was proven that the device is perfectly capable of reducing the base shear, overturning moment and floor acceleration of the frame structure [93].

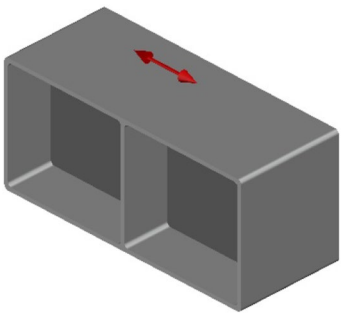

Fig. 10 The aluminum shear-yielding damper

4.3 Lead Dampers

Engineers find lead a favorable dissipation material due to its unique characteristics, including rapid recrystallization at room temperature and high-cycle fatigue life. The first lead dampers were introduced by Robinson and Greenbank [94] with two different configurations. As Fig. 11a illustrates, the first damper is the constricted-tube extrusion energy absorber, which contains two concentric cylinders. Lead is enclosed by the inner cylinder, while the outer cylinder has an orifice around its mid-length. The inner cylinder is separated by a thin lubricant layer for the movement of the piston within the outer tube. The outer cylinder is fixed while the inner shaft is loaded axially. As the shaft moves back and forth, the lead extrudes back and forth through the outer cylinder's orifice. Figure 11b shows the second lead damper configuration, named the bulged-shaft extrusion energy absorber, which works with the same principle. The damper has a central shaft with a bulge in the middle. The central shaft is surrounded by lead with bearings at both sides to grip the lead in place. The bulge section extrudes the lead material as the central piston is loaded. As the shaft moves in the tube, the lead extrudes back and forth through the orifice formed by the bulge. Thereby, the energy dissipates through the extrusion of the lead material, causing plastic deformation in the lead. Lead dampers are dependent on operating temperature. Lead recrystallization occurs below 20 °C; hence, lead dampers are able to recover and recrystallize rapidly. Soydan et al. [95] tested the application of the extrusion damper in steel connections. The results indicated that the restoring force of the connection significantly improved after damper implementation. In addition, the connection displacement reduced substantially compared to the bare connection. Curadelli and Riera [96] developed the ringed-type lead damper, as demonstrated in Fig. 11c. The damper consists of two concentric cylinders. The inner cylinder has several lead ring sections attached to a shaft. As the shaft end moves back and forth, the lead in the rings is subjected to shear and compressive stresses. Plastic deformation occurs as the rings deform. Cheng et al. [97] presented the clapboard-type lead damper. The lead material is clamped between several steel slots, and the slots are hinged to the top and bottom plates (Fig. 11d). Two steel plates are provided on the damper sides to prevent the squeezing out of the lead material during seismic loading. Experimental and numerical studies have proven that the proposed damper exhibits low yield displacement and excellent energy dissipation capability under different types of dynamic loading.

4.4 Copper Dampers

The characteristics of copper are high ductility, low yield capacity and corrosion resistance. Copper in the shape of an hourglass was suggested as an energy dissipation device by de la Llera et al. [98] and Briones and Llera [99]. It can be seen in Fig. 12 that the copper damper is highly dependent on the aspect ratio of its height to the middle hourglass thickness. The copper damper is more efficient during non-impulsive ground motions and less efficient when the structure enters the inelastic range. Copper dampers have been analyzed experimentally and numerically to construct a constitutive model and produced large numbers of fat hysteresis loops with low yield displacement.

4.5 Shaped Memory Alloy Dampers

Shape memory alloy (SMA) is effective in energy dissipation systems due to a number of advantages, including superelasticity, shape memory effect, low and high fatigue life, high damping, corrosion resistance, and young's

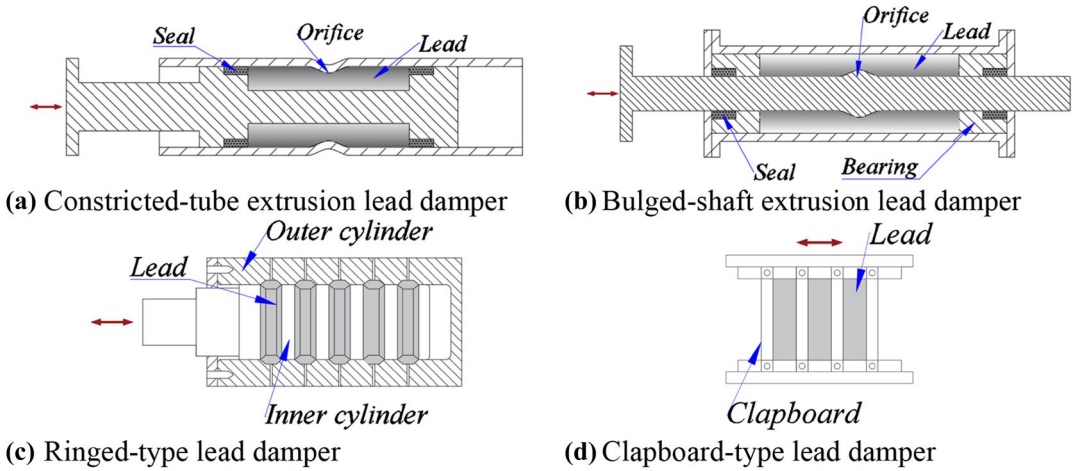

(a) Constricted-tube extrusion lead damper
(b) Bulged-shaft extrusion lead damper
(c) Ringed-type lead damper
(d) Clapboard-type lead damper

Fig. 11 Lead dampers

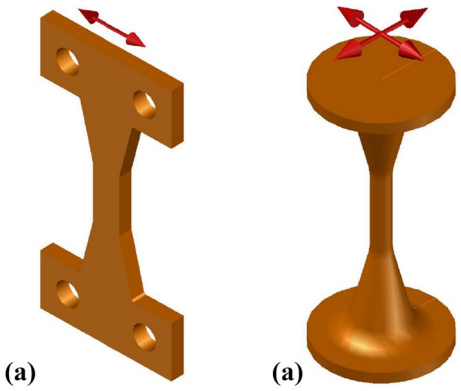

Fig. 12 Copper dampers, **a** plate and **b** round hourglass dampers

modulus-temperature relations. SMA is able to tolerate large strains with no signs of residual deformation when it is unloaded. Casciati et al. [100] proposed an SMA frame damper made of three vertical steel columns connected to each other by an SMA beam as illustrated in Fig. 13a. The two outer legs are anchored to the bridge deck while the middle leg is attached to the vibration source. The damper shows good ductility and service life for bridge applications. DesRoches and Delemont [16] presented a round SMA energy dissipation device for bridge applications (Fig. 13b). The proposed damper is installed between the bridge deck and the pier to enhance the seismic performance of the bridge. Sepúlveda et al. [101] proposed a bar-shaped damper using a combination of copper and SMA to take advantage of both materials for energy dissipation. The copper-based SMA damper performance was evaluated through the shaking table test while it was installed in a beam-to-column connection. Zhang and Zhu [102] proposed a reusable hysteretic damper (RHD) composed of two sliding steel blocks with Teflon sheets laid between them. Each block has two anchor fixtures to hold the pre-stressed SMA wires (Fig. 13c). The damper may be adjusted for several sets of SMA wires according to the required configuration. Moreover, the proposed RHD can be reused even after earthquake events owing to its long-term reliability.

Dolce et al. [103] proposed a self-centering SMA-based energy dissipating device made of two concentric steel pipes and several studs inserted between them. Four sets of SMA wires are connected to the studs: two sets are re-centering wire loops and the two other sets are dissipating wire loops as shown in Fig. 14a. The re-centering SMA wires are pre-tensioned according to the required force in order to bring the device back to the initial position. The device performance was tested in the bracing system of a concrete frame, where the tension and compression forces were dissipated by SMA wires [104]. The device enhanced the frame performance and helped the frame to have minimal residual displacement after an earthquake event. Figure 14b shows another type of self-centering SMA-based damper proposed by Ma et al. [105, 106] that consists of five groups: i.e., internal shaft group, external tube group, SMA wire group,

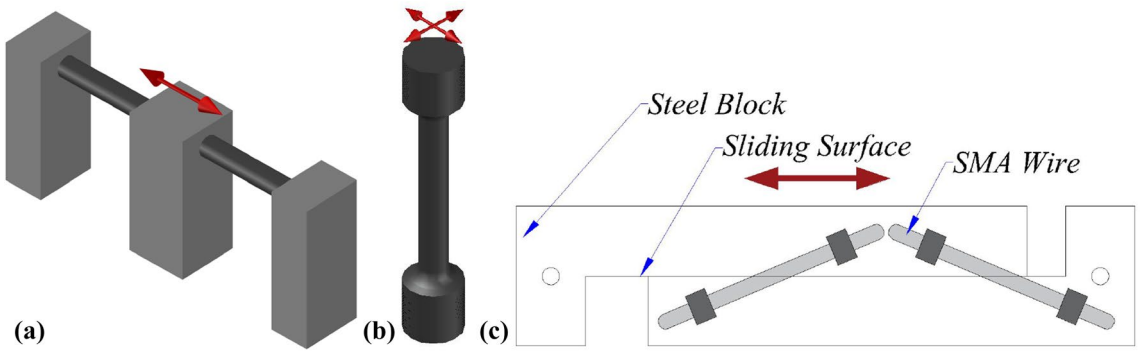

Fig. 13 Schematic views of **a** SMA frame damper, **b** SMA bar damper and **c** RHD

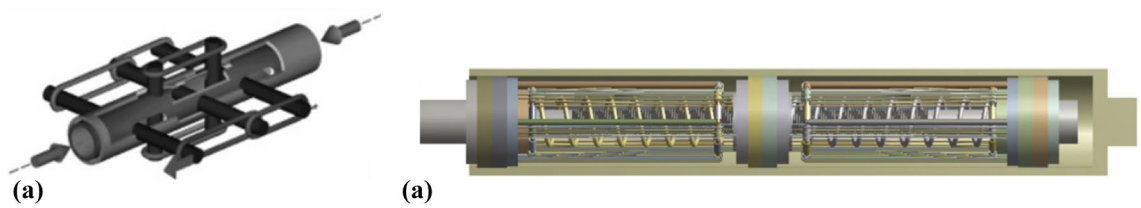

Fig. 14 Schematic view of self-centering SMA dampers [103, 105]

springs, and roller system connection group. The internal shaft group is composed of a shaft with two moveable shim plates at the ends and one anchor fixed in the middle. The external tube group consists of a steel tube with two anchors at both ends. The two pre-compressed springs are connected to the middle fixed anchor and the shim plates, while the springs surround the pre-tensioned SMA wires. The damper benefits from the energy dissipation capability of the spring and SMA groups. It exhibits full re-centering capability, a high number of working cycles and excellent damping ratio.

5 Computational Methods

Nowadays, various computational methods are commonly used in the development and evaluation of the metallic dampers either solely or together with the primary structures [107]. Computational methods significantly reduce the time and cost of the investigation. Broadly speaking, computational methods used in the analysis of metallic dampers are classified into three categories i.e., advanced finite element programs, structural analysis programs and programming languages. These programs may be utilized individually or combined together for various goals in the development and investigation of metallic dampers. The following sections describe each category with the respective examples used for the analysis of metallic dampers.

5.1 Advanced Finite Element Programs

Advanced finite element programs (such as ABAQUS, ANSYS, LS-DYNA, Solidworks, etc.) are the most used computational methods in developing metallic dampers. These programs are rigorously able to model the metallic dampers with the primary structures. These programs are usually used for preliminary design and analysis of metallic dampers [63, 64, 72] or the extension of experimental investigation [68, 80, 82]. In addition, the primary structures equipped with metallic dampers can be modelled in the mentioned programs, however, it requires a profound modeling knowledge and high-performance computers. In addition, different material modeling with different damage criteria are available to simulate the hysteresis behavior of metallic dampers. A large numbers of studies on metallic dampers were performed by ABAQUS [58, 62, 68, 73, 74, 76, 81–83, 109–111] and ANSYS [54, 59, 64, 66, 85, 91, 112, 113] software.

Dongbin et al. [48] modeled the CBRB with a four-node shell element with reduced integration in ABAQUS program as shown in Fig. 15. In order to simulate the metal behavior under cyclic loadings, it is a common practice to use the following back stress formula:

$$\alpha = \sum_{k=1}^{n} \frac{C_k}{\gamma_k}\left(1 - e^{-\gamma_k \varepsilon^{-pl}}\right) \tag{1}$$

where α is the back stress, $\sum {C_k}/{\gamma_k}$ is the ultimate kinematic hardening stress and ε^{-pl} is the equivalent plastic strain. As Fig. 16a shows, the results of coupon test from the experimental and numerical analysis is well-agreed, which also shows the effectiveness of the material modeling in ABAQUS program. The numerical force–displacement hysteresis curves of damper were also had a close relationship with experimental results (Fig. 16b illustrates the hysteresis curves for one of CBRB specimen). After the validation of models, the effect of the several parameters on the performance of CBRB was investigated with help of the numerical simulation.

Deng et al. [124] used the shape optimization method to enhance the hysteresis performance of U-shaped damper under bidirectional deformation. As Fig. 17a shows, the U-shaped damper was modelled with an 8-node, reducing integration with an hourglass, controlled linear brick element. The cyclic behavior of steel was calculated from the back stress formula (Eq. 1). From the obtained results, it was found that the width and length of the straight part of the U-shaped damper (b_2, l) govern the damper stiffness. The shape optimization method used based on the obtained results and the design variables were chosen as the width and length of the straight part of the damper. The design parameters were used as the objective function of the optimization process:

$$\begin{cases} \textit{Design parameters} & b_2, l \\ \textit{Maximize} & {ALLPD}/{PEEQ_{max}^{0.6}} \end{cases} \tag{2}$$

where ALLPD is the energy dissipated plastic deformation and PEEQ is an equivalent plastic strain. Figure 17b demonstrates the flowchart of the optimization process. The

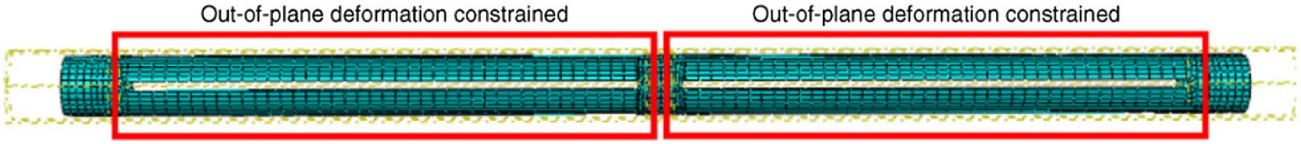

Fig. 15 BRB finite element model in ABAQUS program [48]

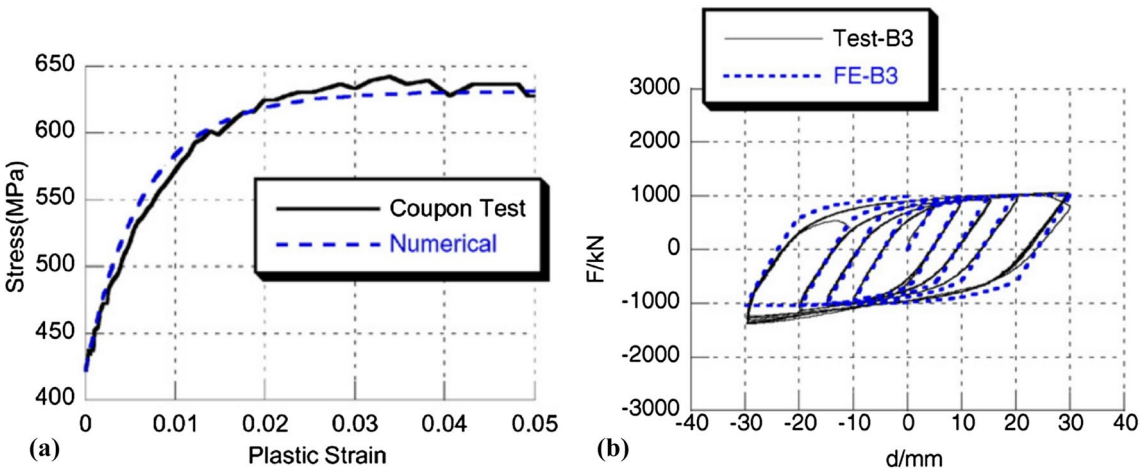

Fig. 16 **a**Stress–strain curve from coupon test and **b** hysteresis curves of CBRB [48]

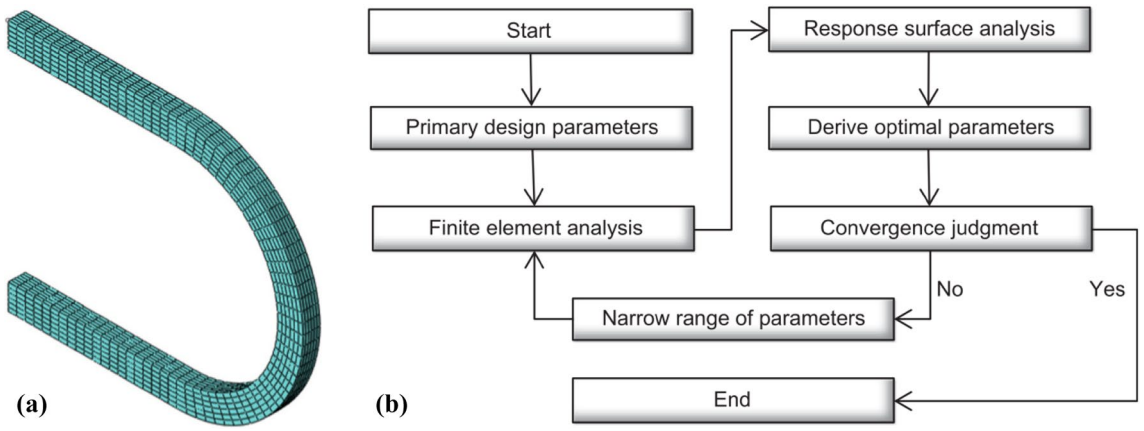

Fig. 17 **a** FE discretization of C-shaped damper in ABAQUS program and **b** the proposed optimization process flowchart [124]

Matlab programming code used for surface analysis and convergence of the optimization analysis. As a conclusion, the optimal design parameters were obtained that maximized the total energy dissipation capacity of the U-shaped damper.

Usami et al. [125] investigated the implementation of BRBs for seismic performance upgrading of steel arch bridges. Three-dimensional models of the bridge were created in ABAQUS program. The girders, columns and deck slabs were model with the Timoshenko beam element. The dummy element was employed to model the reinforced concrete deck. A bilinear stress–strain curve with kinematic hardening rule was employed for the steel members. Only, the stress–strain curve of the concrete in compression was assigned to the concrete members. Two seismic performance upgrading configurations were purposed as shown in Fig. 18. The bridge models were subjected to several earthquake excitations and the results showed that the bridges with BRBs had satisfactory seismic performance. It was also found that the usage of BRB is an efficient alternative in seismic retrofitting of existing steel arch bridges.

Aghlara and Tahir [90] extended the experimental investigation of the BFD using ANSYS program. Owing to the symmetry of the damper in two planes, only a quarter of the geometry of the damper was modelled as shown in Fig. 19. All parts of the BFD modelled as the solid element and appropriate boundary conditions, as well as required interactions, were defined for the model. The results of finite element analysis had a close correlation with the experimental results.

The clapboard-type lead damper was modelled as an eight-nodal 3D solid element in ANSYS program as shown in Fig. 20a [98]. The lead material was modeled using elastic–plastic kinematic hardening rule. The hysteresis curves of simulation analysis had a slight difference with experimental curves due to simplification of the lead material in modeling. In order to evaluate the effectiveness of the

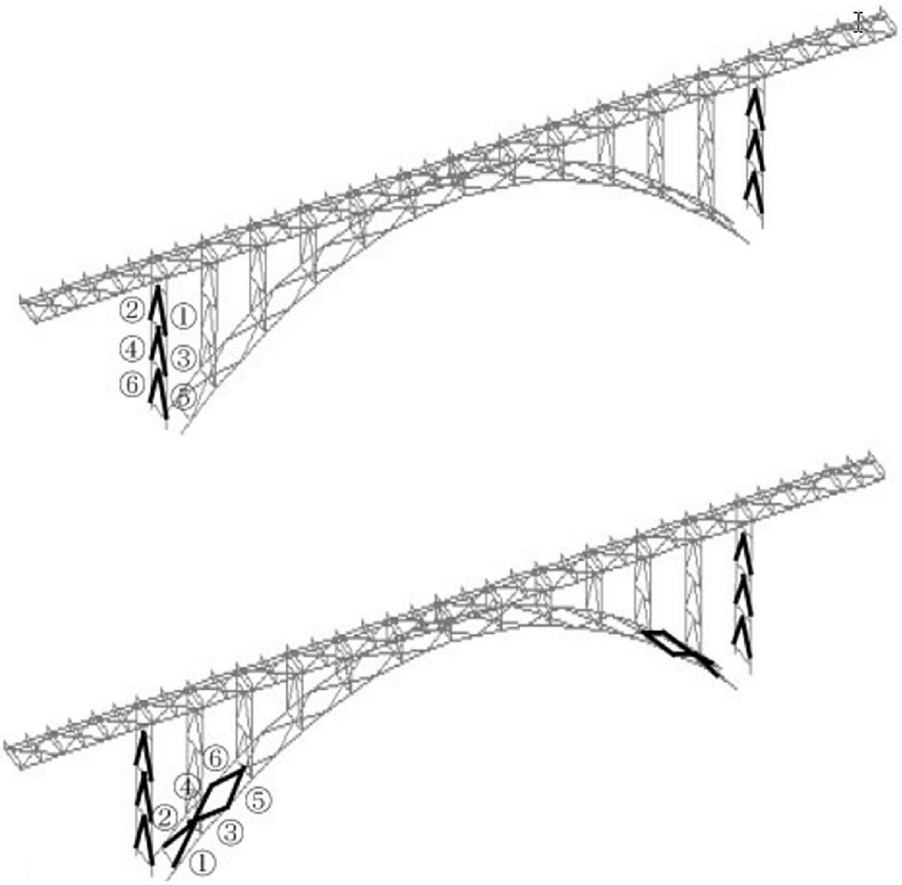

Fig. 18 Steel arch bridge models retrofitted with BRBs in ABAQUS program [125]

proposed damper, a 20 storey Benchmark building equipped with the dampers were modelled and analyzed through nonlinear time-history analysis as shown in Fig. 20b. The beams and columns were modelled with the beam element while the lead dampers were modelled with the spring combination element. The results of numerical analysis showed that the top storey acceleration and displacement of the benchmark building with dampers were reduced by 26.7% and 37.4% as compared to the uncontrolled building, respectively.

5.2 Structural Analysis Programs

Generally, structural engineers investigate the application of metallic dampers in building and bridge structures using commercial structural analysis programs such as SAP2000 [47, 57, 84, 96, 114–116] Perform 3D [115–117], Etabs, CSiBridge and others. These programs are employed when the metallic damper application should be tested in megastructures where the feasibility of the experimental test is difficult. The characteristics of the dampers are modelled by the different elements in these programs and nonlinear time-history analysis is the most common practice analysis to evaluate the dampers effectiveness.

Shen et al. [126] developed three dimensional numerical model of Transverse Steel Damper (TSD) in ABAQUS and validated it with experimental results. Thereafter, the application of TSD was examined in a long span cable-stayed bridge using SAP2000 program. The towers, RC piers and steel box girders were modelled with the elastic beam element while the truss element used for modeling the cables as shown in Fig. 21. The link element with Wen Plasticity property was deployed to model the metallic dampers and sliding bearings. The Hilber-Hughes-Taylor time integration solver was employed for nonlinear time-history analysis of 29 earthquake excitations. In conclusion, the TSD system reduced the transverse displacement of the cable-stayed bridge and dissipated a large amount of seismic energy as compared to sliding bearings.

Li et al. [127] examined the effectiveness of BRBs as metallic fuse dampers in an existing school building in China using SAP2000 program. As Fig. 22 illustrated, the BRBs was implemented in side-frames of the building that led to the improvement of the lateral and torsional stiffness of the bays. The Wen Plasticity property type was deployed in modelling the BRBs. The results of modal and pushover analyses showed that the stiffness and ductility of the building significantly increased after the implementation

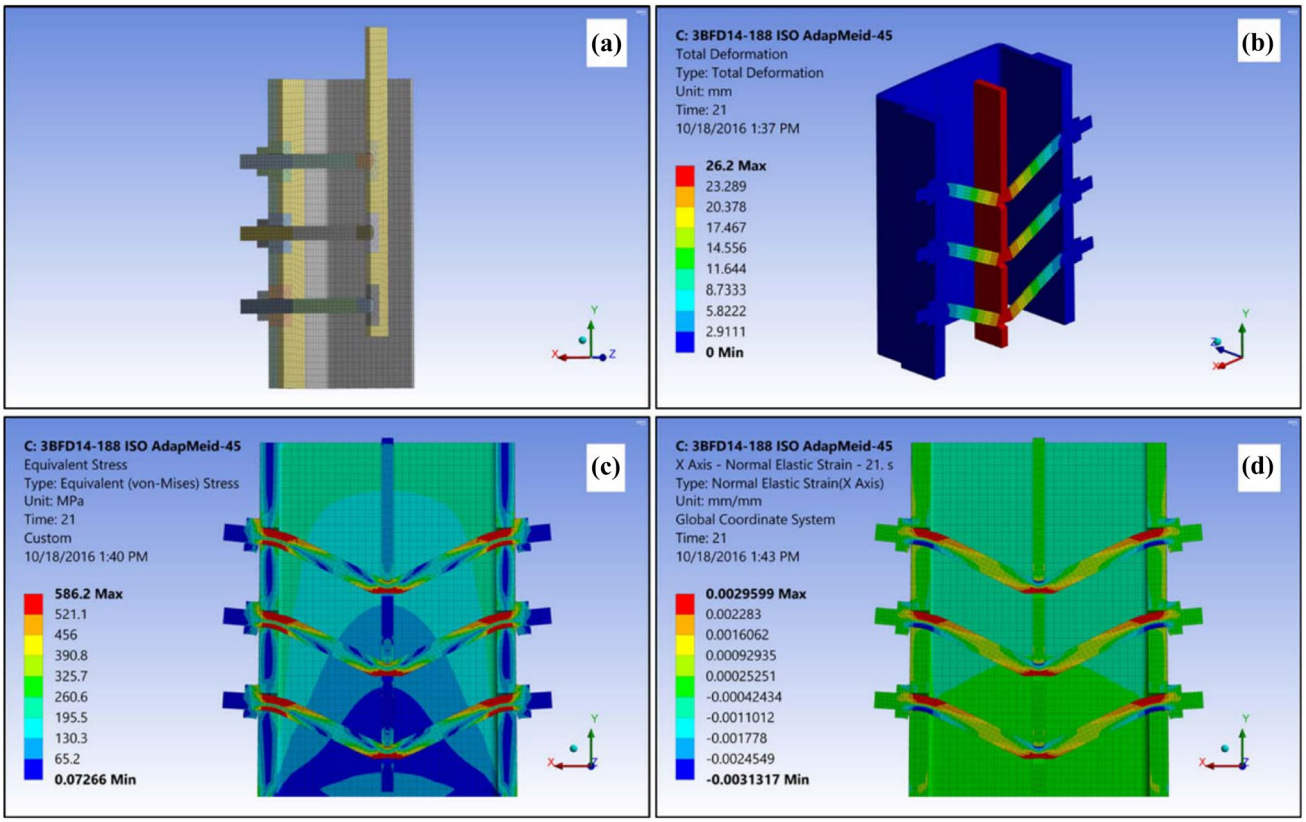

Fig. 19 Finite element model and results of BFD in ANSYS Program [88]

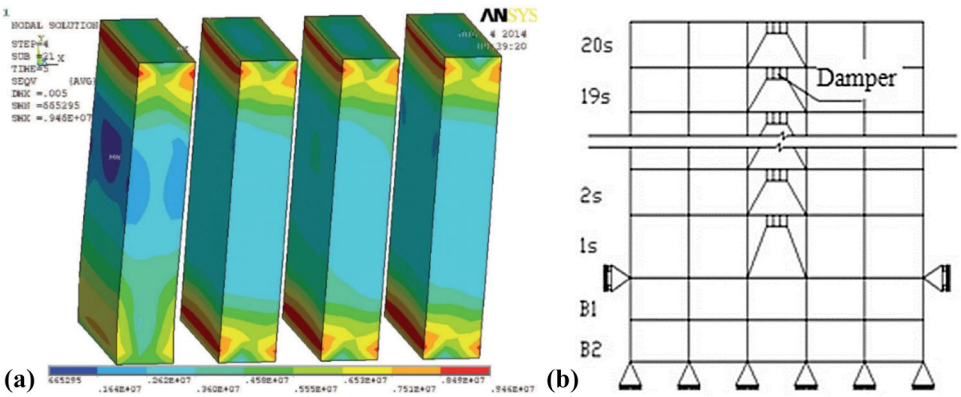

Fig. 20 **a** Stress distribution pattern of clapboard lead damper in ANSYS program and **b** installation scheme of clapboard lead dampers in 20-story benchmark building [96]

of BRBs. It was also reported that all the members of the main frame remained elastic in the nonlinear time-history analysis.

5.3 Programming Languages

Programming languages such as OpenSees, IDARC-2D, Matlab, FORTRAN among others are another tools used to investigate the effectiveness of metallic dampers [100, 120–123]. These programming codes need a deep programming knowledge for the modelling and analysis.

Ma and Yam [107] assessed the self-centering SMA damper behavior through Matlab/Simulink environment. The hysteresis behavior of the SMA was modeled using the Bouc–Wen model and the re-centering group was modelled with Coulomb and Viscous Friction function. The damper response subjected to three-sine-wave displacement excitations was evaluated according to the flowchart shown in Fig. 23. The equation of motion for the structure (a

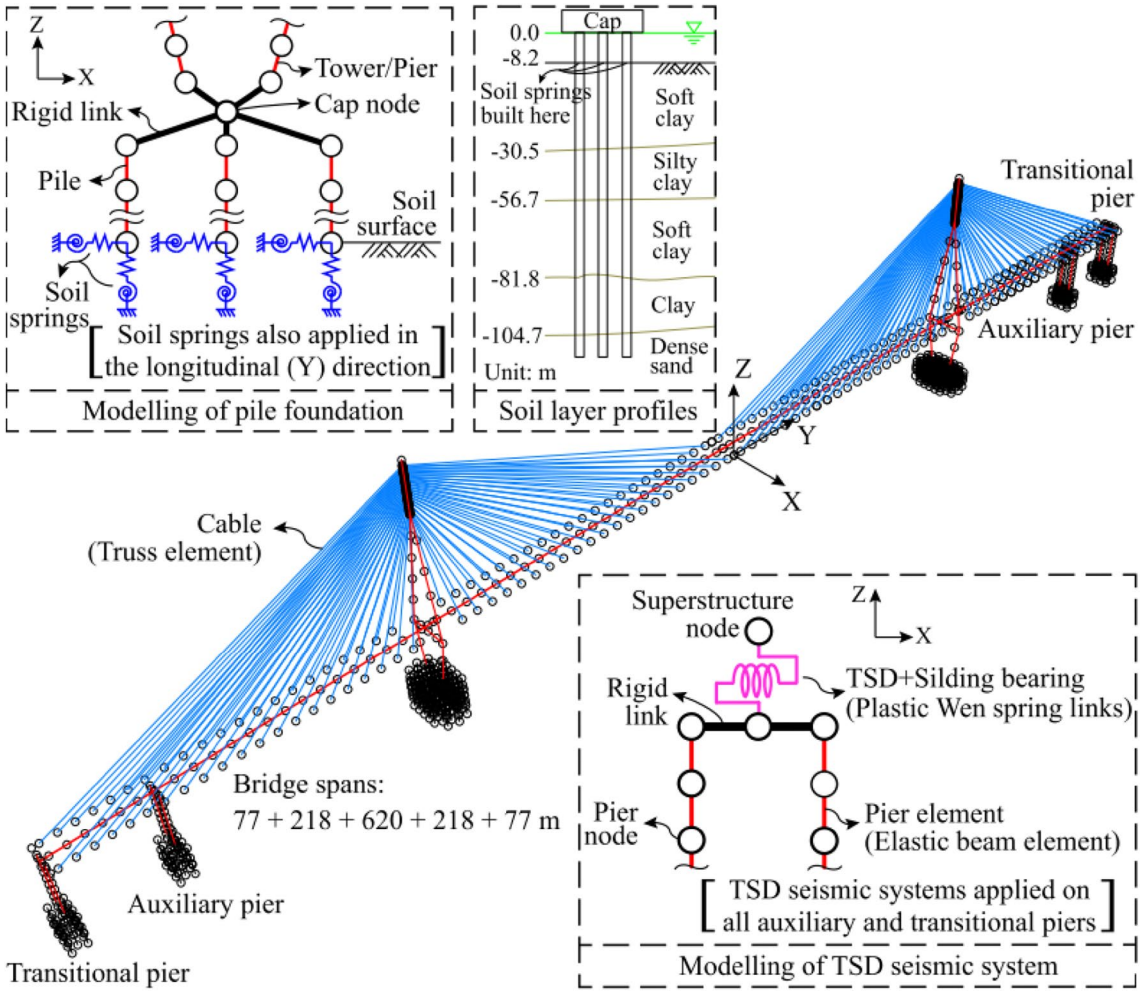

Fig. 21 3D modelling of the cable-stayed bridge with TSDs in SAP2000 program [126]

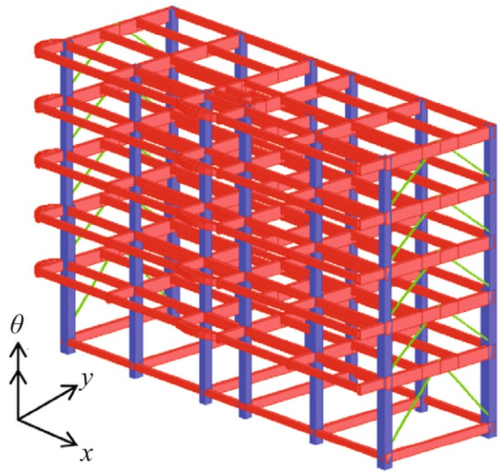

Fig. 22 Implementation of BRBs in school building using SAP2000 program [127]

single-degree-of-freedom) equipped with the SMA damper subjected to earthquake excitation is:

$$[M]\{\ddot{x}\} + [C]\{\dot{x}\} + [K]\{x\} + [\Gamma]\{x\} = -[M]\{\ddot{x}_g\} \quad (3)$$

where [M], [C] and [K] are the structure mass, damping and stiffness matrix, respectively. Vector {x} is the lateral displacement. The [Γ] is the generic integral–differential operator matrix. [Γ]{x} is the control force generated by the SMA damper and $\{\ddot{x}_g\}$ is the earthquake acceleration vector.

A 1/4-scale five-storey steel frame was modelled in ANSYS program and verified with earlier results of shaking table test on the porotype structure [107]. The mass, damping and stiffness matrix were obtained from the ANSYS program and used to construct the equivalent lumped mass model of the steel frame for the dynamic analysis (see Fig. 24a) in Matlab/Simulink environment based on the flowchart shown in Fig. 24b. The results of nonlinear time-history analysis indicated that the inter-storey drift and floor displacement reduced for the steel frame with the

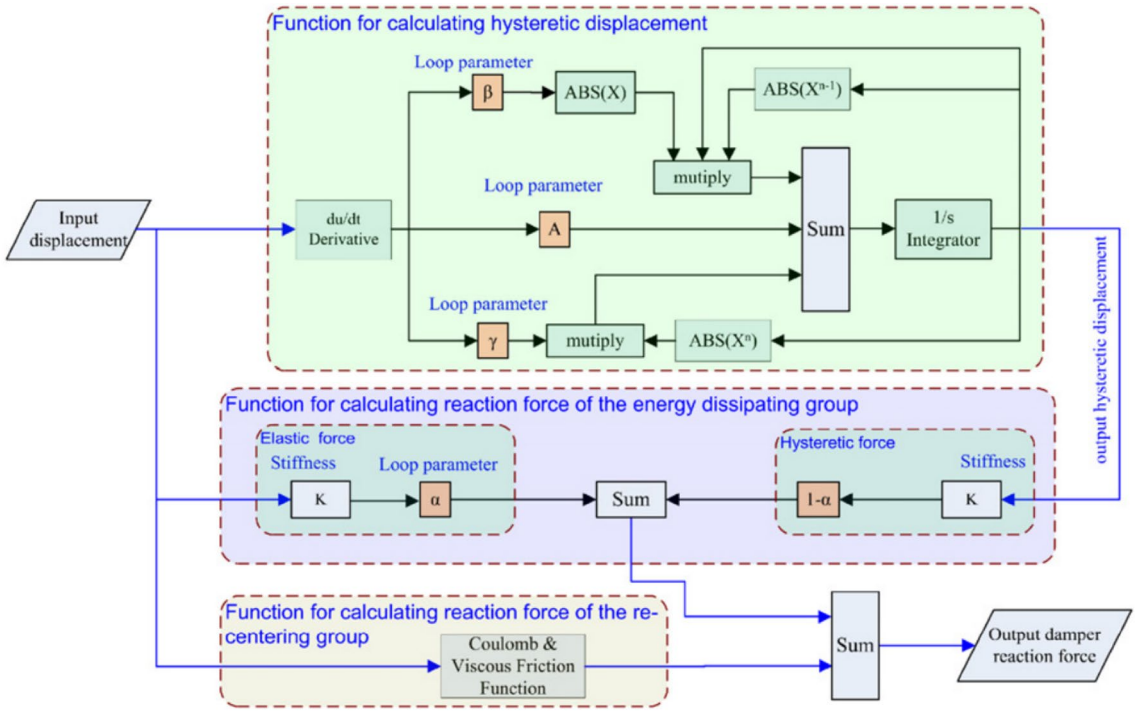

Fig. 23 Matlab/Simulink block procedure for determining the SMA damper characteristics [107]

re-centering SMA damper and no sign of residual deformation observed after earthquake excitations.

6 Application

Metallic damper configurations may be altered to achieve the design requirements of engineers for mitigating dynamic loads in various types of structures [128]. Metallic dampers may be implemented in flexible frames, as a connecting element between the frame and rigid tower, in structures with a stepping tower and in base-isolated structure as illustrated in Fig. 25a–d [32, 39, 129, 130]. ADAS dampers are recommended to be used in moment resisting frames such as the chevron bracing system, and thereafter, a large number of other metallic dampers are also suggested to be used in the same location for concrete or steel frame systems [49, 130–132]. The conventional bracing system may not be adequate for dynamic loadings; hence, metallic dampers have been used in addition to the conventional bracing (e.g. diagonal and X-type) as depicted in Fig. 25e–g [42, 55]. Dampers may also be used as shear walls to enhance the seismic performance of frames. In addition, it has been recommended to install a metallic damper in the middle of a secondary column (inner column) to increase the lateral stability of the frame system (Fig. 25h) [67, 68]. Tagawa et al. [133] suggested placing metallic dampers in various configurations of the seesaw bracing system (Fig. 25i–k). Utilizing metallic dampers in the beam-to-column connections of moment resisting structures is advantageous, as they provide large openings in the frame bays (Fig. 25l) [60, 64, 81]. Nonetheless, metallic dampers can also be installed between decks and piers or abutment of the bridges in the principal and transverse directions (Fig. 25m) [76, 86, 109, 114, 116]. Various applications of dampers in different structures are shown schematically in Fig. 25.

7 Concluding Remarks

This paper outlined a comprehensive state-of-art review of metallic dampers since the 1970s. The damper classification is based on the following constitutive material: steel, aluminum, lead, copper and SMA dampers. Moreover, the application and analysis of the metallic dampers has been investigated by various computational methods. Steel dampers appear to be among the most popular due to the low manufacturing cost and excellent performance in mitigating structural vibration. Furthermore, after the constitutive material, the damper geometry has significant effects on damper performance. Another important factor during manufacturing of metallic dampers is the welding quality that can prevent premature damper failure during operation. Steel dampers act as fuses in civil structures. In case of failure, they can be easily replaced that prevent

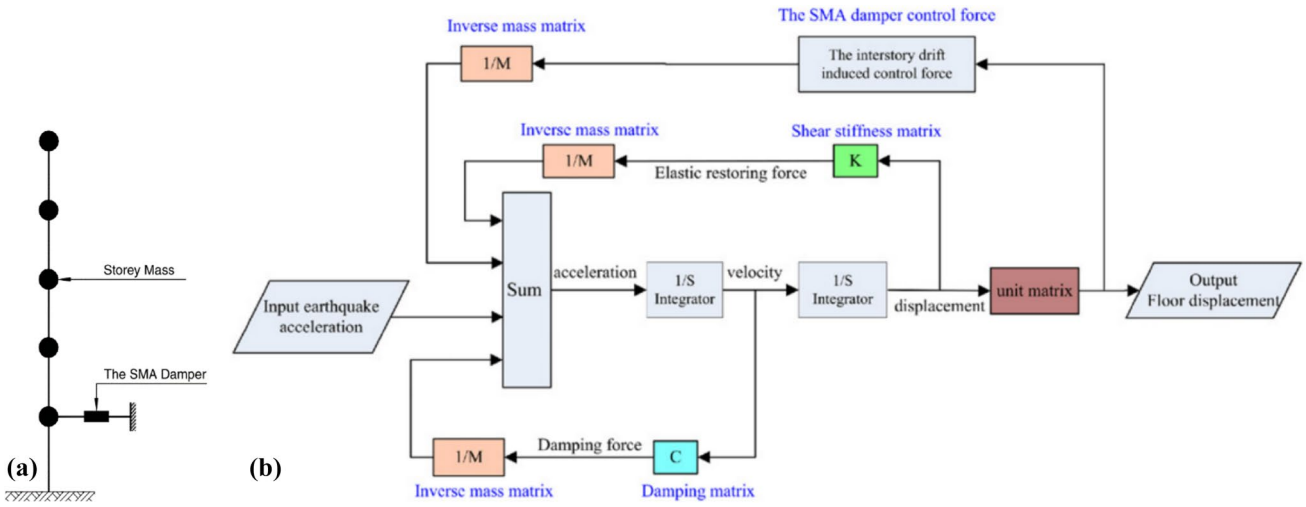

Fig. 24 **a** Equivalent lumped-mass model deployed in Matlab/Simulink and **b** Matlab/Simulink block dynamic analysis procedure for the structure with SMA damper [107]

damage to the primary structures. Aluminum damper with the same geometric configuration as steel damper performed slightly better. The lead damper mechanism is based on the extrusion of the lead material. Lead dampers do not require replacement or repair after earthquake events due to the lead material recrystallization. However, they are expensive and heavier than steel dampers. Copper dampers are not so attractive since copper material is quite a bit costlier than other metals. The use of SMA dampers has been increasing in recent years due to their unique characteristics. Moreover, SMA dampers have relatively higher life cycles than other metallic dampers. In contrast, the initial cost of SMA dampers is much higher. It is also concluded that metallic dampers can be implemented in new structures or retrofitting of the existing structures as one of the most economical alternatives. Ultimately, the use of metallic dampers is fully acknowledged, while the primary mission is to develop and standardize prototype specifications for relevant standards.

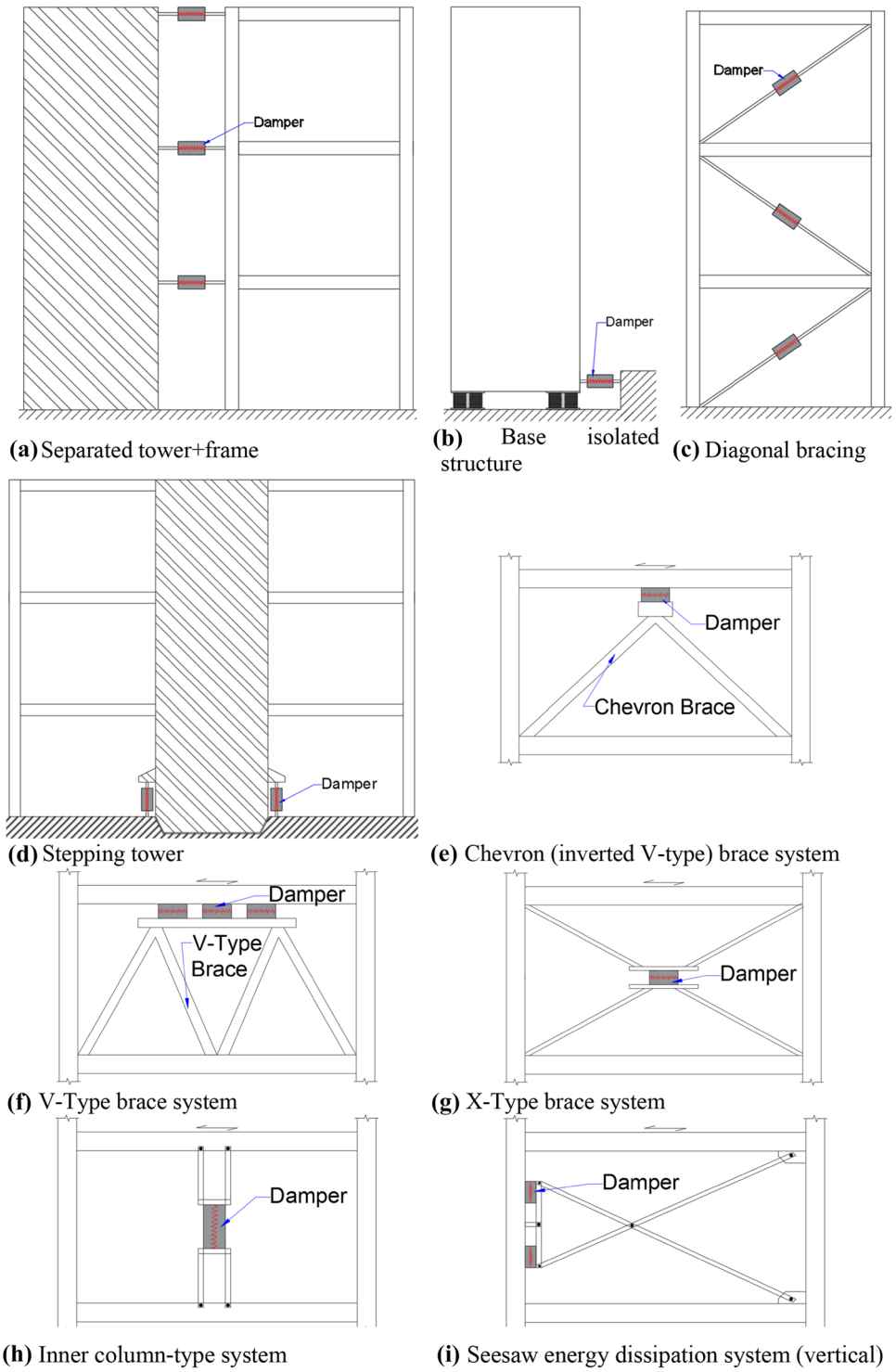

Fig. 25 Schematic locations for the installation of metallic dampers in civil structures

Fig. 25 (continued)

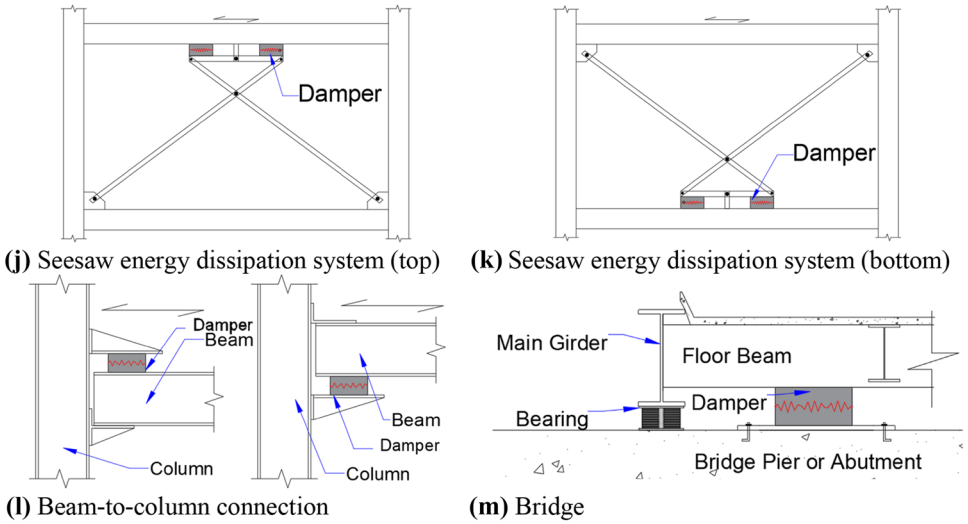

(j) Seesaw energy dissipation system (top) **(k)** Seesaw energy dissipation system (bottom)

(l) Beam-to-column connection **(m)** Bridge

Acknowledgements The authors gratefully acknowledge the supported given by University Malaya Research Grant (UMRG—Project No. RP004A/13AET).

Compliance with Ethical Standards

Conflict of interest On behalf of all authors, the corresponding author states that there is no conflict of interest.

References

1. Ghaedi K, Ibrahim Z (2017) Earthquake prediction. In: Zouaghi T (ed) Earthquakes—tectonics, hazard risk mitigation. InTech, London, pp 205–227. https://doi.org/10.5772/65511
2. Spencer BF Jr, Nagarajaiah S (2003) State of the art of structural control. J Struct Eng 129:845–856
3. Saaed TE, Nikolakopoulos G, Jonasson J-E, Hedlund H (2013) A state-of-the-art review of structural control systems. J Vib Control 21:919–937. https://doi.org/10.1177/1077546313478294
4. Housner GW, Bergman LA, Caughey TK, Chassiakos AG, Claus RO, Masri SF, Skelton RE, Soong TT, Member S, Spencer BF, Yao JTP (1997) Structural control: past, present, and future. J. Eng. Mech. 123:897–971
5. Soong TT, Spencer BF (2002) Supplemental energy dissipation: state-of-the-art and state-of-the- practice. Eng Struct 24:243–259. https://doi.org/10.1016/S0141-0296(01)00092-X
6. Symans MD, Charney FA, Whittaker AS, Constantinou MC, Kircher CA, Johnson MW, McNamara RJ (2008) Energy dissipation systems for seismic applications: current practice and recent developments. J Struct Eng 134:3–21. https://doi.org/10.1061/(asce)0733-9445(2008)134:1(3)
7. Li H, Huo L (2010) Advances in structural control in civil engineering in China. Math Probl Eng. https://doi.org/10.1155/2010/936081
8. Fisco NR, Adeli H (2011) Smart structures: part I—active and semi-active control. Sci Iran 18:275–284. https://doi.org/10.1016/j.scient.2011.05.034
9. Fisco NR, Adeli H (2011) Smart structures: part II—hybrid control systems and control strategies. Sci Iran 18:285–295. https://doi.org/10.1016/j.scient.2011.05.035
10. Korkmaz S (2011) A review of active structural control: challenges for engineering informatics. Comput Struct 89:2113–2132. https://doi.org/10.1016/j.compstruc.2011.07.010
11. El-Khoury O, Adeli H (2013) Recent advances on vibration control of structures under dynamic loading. Arch Comput Methods Eng 20:353–360. https://doi.org/10.1007/s11831-013-9088-2
12. Ghaedi K, Ibrahim Z, Adeli H, Javanmardi A (2017) Invited Review: recent developments in vibration control of building and bridge structures. J VibroEng 19:3564–3580. https://doi.org/10.21595/jve.2017.18900
13. Gutierrez Soto M, Adeli H (2013) Tuned mass dampers. Arch Comput Methods Eng. 20:419–431. https://doi.org/10.1007/s11831-013-9091-7
14. Di Sarno L, Elnashai AS (2005) Innovative strategies for seismic retrofitting of steel and composite structures. Earthq Eng Struct Dyn 7:115–135. https://doi.org/10.1002/pse.195
15. Dargush GF, Sant RS (2005) Evolutionary aseismic design and retrofit of structures with passive energy dissipation. Earthq Eng Struct Dyn 34:1601–1626. https://doi.org/10.1002/eqe.497
16. DesRoches R, Delemont M (2002) Seismic retrofit of simply supported bridges using shape memory alloys. Eng Struct 24:325–332. https://doi.org/10.1016/S0141-0296(01)00098-0
17. Javanmardi A (2014) Non-linear test of precast subframe subjected to cyclic lateral loadings. Universiti Teknologi Malaysia
18. Javanmardi A, Abadi R, Marsono AK, Tap M, Ibrahim Z, Ahmad A (2015) Correlation of stiffness and natural frequency of precast frame system. Appl Mech Mater 735:141–144. https://doi.org/10.4028/www.scientific.net/AMM.735.141
19. Ghaedi K, Ibrahim Z, Jameel M, Javanmardi A, Khatibi H (2018) Seismic response analysis of fully base isolated adjacent buildings with segregated foundations. Adv Civ Eng. https://www.hindawi.com/journals/ace/aip/4517940/
20. Javanmardi, A., Ibrahim, Z., & Ghaedi, K. (2018, October). Development of a new hybrid precast beam-to-column connection. In IOP Conference Series: Materials Science and Engineering (Vol. 431, No. 11, p. 112002). IOP Publishing.
21. Prucz JC, Kokkinos F, Spyrakos CC (1989) Advanced joining concepts for passive vibration control. J Aerosp Eng 1:193–205
22. Ali HM, Abdel-Ghaffar AM (1995) Modeling of rubber and lead passive-control bearings for seismic

analysis. J Struct Eng 121:1134–1144. https://doi.org/10.1061/(ASCE)0733-9445(1995)121:7(1134)
23. Tirca LD, Foti D, Diaferio M (2003) Response of middle-rise steel frames with and without passive dampers to near-field ground motions. Eng Struct 25:169–179. https://doi.org/10.1016/S0141-0296(02)00132-3
24. Ibrahim RA (2008) Recent advances in nonlinear passive vibration isolators. J Sound Vib 314:371–452. https://doi.org/10.1016/j.jsv.2008.01.014
25. Parulekar YM, Reddy GR (2009) Passive response control systems for seismic response reduction: a state-of-the-art review. Int J Struct Stab Dyn 9:151–177
26. Martinelli P, Mulas MG (2010) An innovative passive control technique for industrial precast frames. Eng Struct 32:1123–1132. https://doi.org/10.1016/j.engstruct.2009.12.038
27. Javanmardi A, Ghaedi K, Ibrahim Z, Khatibi H (2016) Nonlinear seismic behavior of a based isolated cable-stayed bridge. In: Shahid Beheshti University (ed) 4th international congress on civil engineering, architecture and urban development, Civilica, Tehran. https://www.civilica.com/Paper-ICSAU04-ICSAU04_0204.html
28. Javanmardi A, Ibrahim Z, Ghaedi K, Jameel M, Khatibi H, Suhatril M (2017) Seismic response characteristics of a base isolated cable-stayed bridge under moderate and strong ground motions. Arch Civ Mech Eng 17:419–432. https://doi.org/10.1016/j.acme.2016.12.002
29. Javanmardi A, Ibrahim Z, Ghaedi K, Jameel M, Usman H, Gordan M (2018) Seismic response of a base isolated cable-stayed bridge under near-fault ground motion excitations. Sci Res J 15:1–14
30. Javanmardi A, Ibrahim Z, Ghaedi K, Khan NB, Ghadim HB (2018) Seismic isolation retrofitting solution for an existing steel cable-stayed bridge. PLoS ONE 13:1–22. https://doi.org/10.1371/journal.pone.0200482
31. Wang JN, Munfakh GA (2014) Buildings and bridges equipped with passive dampers under seismic actions: modeling and analysis. Encycl Earthq Eng. https://doi.org/10.1007/978-3-642-36197-5
32. Skinner RI, Kelly JM, Heine AJ (1974) Hysteretic dampers for earthquake-resistant structures. Earthq Eng Struct Dyn 3:287–296. https://doi.org/10.1002/eqe.4290030307
33. Kobori T, Miura Y, Fukuzawa E (1992) Development and application of hysteresis steel dampers. In: Tenth world conference on earthquake engineering, pp 2341–2346
34. Nakashima M, Saburi K, Tsuji B (1996) Energy input and dissipation behaviour of structures with hysteretic dampers. Earthq Eng Struct Dyn 25:483–496. https://doi.org/10.1002/(SICI)1096-9845(199605)25:5%3c483:AID-EQE564%3e3.0.CO;2-K
35. FEMA-416 (2007) Interim testing protocols for determining the seismic performance characteristics of structural and nonstructural components. Federal Emergency Management Agency, Washington, DC (USA)
36. Bannantine JA, Comer JJ, Handrock JL (1990) Fundamental of metal fatigue analysis. Prentice Hall, Englewood Cliffs
37. Azevedo J, Calado L (1994) Hysteretic behaviour of steel members: analytical models and experimental tests. J Constr Steel Res 29:71–94. https://doi.org/10.1016/0143-974X(94)90057-4
38. Miller D, Doh J-H (2014) A simple hybrid damping device with energy-dissipating and re-centering characteristics for special structures. Struct Des Tall Spec Build. 24:421–439. https://doi.org/10.1002/tal
39. Kelly JM, Skinner RI, Heine AJ (1972) Mechanisms of energy absorption in special devices for use in earthquake resistant structures. Bull N Z Natl Soc Earthq Eng 5:63–88
40. Tyler RG (1978) Tapered steel energy dissipators for earthquake resistant structures. Bull N Z Natl Soc Earthq Eng 11:282–294
41. Pinelli JP, Craig JI, Goodno BJ, Hsu C-C (1993) Passive control of building response using energy dissipating cladding connections. Earthq Spectra 9:529–546. https://doi.org/10.1193/1.1585728
42. Y Takeda, Y Kimura, K Yoshioka, N Furuya, Y Takemoto (1976) An experimental study on braces encased in steel tube and mortal. In: Annual meeting architectural Institute of Japan, pp 1041–1042
43. Wada A, Saeki E, Takeuchi T, Watanabe A (1989) Development of unbonded brace, Column, Nippon Steel Publication, p 115
44. Black C, Makris N, Aiken ID (2004) Component testing, seismic evaluation and characterization of buckling-restrained braces. Pacific Earthquake Engineering Research Center. J Struct Eng 130:880–894. https://doi.org/10.1061/(ASCE)0733-9445(2004)130:6(880)
45. Black C, Makris N, Aiken ID (2002) Component testing, stability analysis and characterization of buckling-restrained unbonded braces (TM). Pacific Earthquake Engineering Research Center.
46. Zhao J, Wu B, Ou J (2011) A novel type of angle steel buckling-restrained brace: cyclic behavior and failure mechanism. Earthq Eng Struct Dyn 40:1083–1102. https://doi.org/10.1002/eqe
47. Hao X-Y, Li H-N, Li G, Makino T (2014) Experimental investigation of steel structure with innovative H-type steel unbuckling braces. Struct Des Tall Spec Build 24:421–439. https://doi.org/10.1002/tal
48. Dongbin Z, Xin N, Peng P, Mengzi W, Kailai D, Yabin C (2016) Experimental study and finite element analysis of a buckling-restrained brace consisting of three steel tubes with slotted holes in the middle tube. J Constr Steel Res 124:1–11. https://doi.org/10.1016/j.jcsr.2016.05.003
49. Bergman DM (1987) Evaluation of cyclic testing of steel-plate devices for added damping and stiffness. Department of Civil Engineering, University of Michigan
50. Tsai K-C, Chen H-W, Hong C-P, Su Y-F (1993) Design of steel triangular plate energy absorbers for seismic-resistant construction. Earthq Spectra 9:505–528. https://doi.org/10.1193/1.1585727
51. Shih M-H, Sung W-P, Go C-G (2004) Investigation of newly developed added damping and stiffness device with low yield strength steel. J Zhejiang Univ Sci 5:326–334. https://doi.org/10.1631/jzus.2004.0326
52. Shih M-H, Sung WP (2005) A model for hysteretic behavior of rhombic low yield strength steel added damping and stiffness. Comput Struct 83:895–908. https://doi.org/10.1016/j.compstruc.2004.11.012
53. Han Q, Jia J, Xu Z, Bai Y, Song N (2014) Experimental evaluation of hysteretic behavior of rhombic steel plate dampers. Adv Mech Eng 9:99. https://doi.org/10.1155/2014/185629
54. Li H, Li G (2007) Experimental study of structure with "dual function" metallic dampers. Eng Struct 29:1917–1928. https://doi.org/10.1016/j.engstruct.2006.10.007
55. Chan RWK, Albermani F (2008) Experimental study of steel slit damper for passive energy dissipation. Eng Struct 30:1058–1066. https://doi.org/10.1016/j.engstruct.2007.07.005
56. Ghabraie K, Chan R, Huang X, Xie YM (2010) Shape optimization of metallic yielding devices for passive mitigation of seismic energy. Eng Struct 32:2258–2267. https://doi.org/10.1016/j.engstruct.2010.03.028
57. Karavasilis TL, Kerawala S, Hale E (2012) Hysteretic model for steel energy dissipation devices and evaluation of a

minimal-damage seismic design approach for steel buildings. J Constr Steel Res 70:358–367. https://doi.org/10.1016/j.jcsr.2011.10.010
58. Jie Z, Li A, Tong G (2015) Analytical and experimental study on mild steel dampers with non-uniform vertical slits. Earthq Eng Eng Vib 14:111–123. https://doi.org/10.1007/s11803-015-0010-9
59. Hedayat AA (2015) Prediction of the force displacement capacity boundary of an unbuckled steel slit damper. J Constr Steel Res 114:30–50. https://doi.org/10.1016/j.jcsr.2015.07.003
60. Oh S-H, Kim Y-J, Ryu H-S (2009) Seismic performance of steel structures with slit dampers. Eng Struct 31:1997–2008. https://doi.org/10.1016/j.engstruct.2009.03.003
61. Garivani S, Aghakouchak AA, Shahbeyk S (2016) Numerical and experimental study of comb-teeth metallic yielding dampers. Int J Steel Struct 16:177–196. https://doi.org/10.1007/s13296-016-3014-z
62. Fan S, Ding Z, Du L, Shang C, Liu M (2016) Nonlinear finite element modeling of two-stage energy dissipation device with low-yield-point steel. Int J Steel Struct 16:1107–1122. https://doi.org/10.1007/s13296-016-0029-4
63. Wang Y-P, Chien C-SC (2009) A study on using pre-bent steel strips as seismic energy-dissipative devices. Earthq Eng Struct Dyn 38:1009–1026. https://doi.org/10.1002/eqe
64. Hsu HL, Halim H (2017) Improving seismic performance of framed structures with steel curved dampers. Eng Struct 130:99–111. https://doi.org/10.1016/j.engstruct.2016.09.063
65. Nakashima M, Iwai S, Iwata M, Takeuchi T, Konomi S, Akazawa T, Saburi K (1994) Energy dissipation behaviour of shear panels made of low yield steel. Earthq Eng Struct Dyn 23:1299–1313. https://doi.org/10.1002/eqe.4290231203
66. Abebe DY, Jeong SJ, Getahune BM, Segu DZ, Choi JH (2015) Hysteretic characteristics of shear panel damper made of low yield point steel. Mater Res Innov 19:902–910. https://doi.org/10.1179/1432891714Z.0000000001219
67. Chen Z, Ge H, Usami T (2005) Hysteretic performance of shear panel dampers. Adv Steel Struct 2:1223–1228
68. Chen Z, Ge H, Usami T (2006) Hysteretic model of stiffened shear panel dampers. J Struct Eng 132:478–483. https://doi.org/10.1061/(ASCE)0733-9445(2006)132:3(478)
69. Zhang C, Zhang Z, Zhang Q (2012) Static and dynamic cyclic performance of a low-yield-strength steel shear panel damper. J Constr Steel Res 79:195–203. https://doi.org/10.1016/j.jcsr.2012.07.030
70. Deng K, Pan P, Sun J, Liu J, Xue Y (2014) Shape optimization design of steel shear panel dampers. J Constr Steel Res 99:187–193. https://doi.org/10.1016/j.jcsr.2014.03.001
71. Chan RWK, Albermani F, Kitipornchai S (2008) Evaluation of yielding shear panel device for passive energy dissipation. J Constr Steel Res 91:14–25. https://doi.org/10.1016/j.jcsr.2013.08.013
72. Chan RWK, Albermani F, Kitipornchai S (2013) Experimental study of perforated yielding shear panel device for passive energy dissipation. J Constr Steel Res 91:14–25. https://doi.org/10.1016/j.jcsr.2013.08.013
73. Sahoo DR, Singhal T, Taraithia SS, Saini A (2015) Cyclic behavior of shear-and-flexural yielding metallic dampers. J Constr Steel Res 114:247–257. https://doi.org/10.1016/j.jcsr.2015.08.006
74. Deng K, Pan P, Li W, Xue Y (2015) Development of a buckling restrained shear panel damper. J Constr Steel Res 106:311–321. https://doi.org/10.1016/j.jcsr.2015.01.004
75. Kato S, Kim YB, Nakazawa S, Ohya T (2005) Simulation of the cyclic behavior of J-shaped steel hysteresis devices and study on the efficiency for reducing earthquake responses of space structures. J Constr Steel Res 61:1457–1473. https://doi.org/10.1016/j.jcsr.2005.03.006
76. Deng K, Pan P, Wang C (2013) Development of crawler steel damper for bridges. J Constr Steel Res 85:140–150. https://doi.org/10.1016/j.jcsr.2013.03.009
77. Özkaynak H (2017) Model proposal for steel cushions for use in reinforced concrete frames. KSCE J Civ Eng 21:2717–2727. https://doi.org/10.1007/s12205-017-0477-1
78. Benavent-Climent A (2010) A brace-type seismic damper based on yielding the walls of hollow structural sections. Eng Struct 32:1113–1122. https://doi.org/10.1016/j.engstruct.2009.12.037
79. Benavent-Climent A, Morillas L, Vico JM (2015) A study on using wide-flange section web under out-of-plane flexure for passive energy dissipation. Earthq Eng Struct Dyn 44:657–675. https://doi.org/10.1002/eqe
80. Maleki S, Bagheri S (2010) Pipe damper, part I: experimental and analytical study. J Constr Steel Res 66:1088–1095. https://doi.org/10.1016/j.jcsr.2010.03.010
81. Maleki S, Mahjoubi S (2013) Dual-pipe damper. J Constr Steel Res 85:81–91. https://doi.org/10.1016/j.jcsr.2013.03.004
82. Maleki S, Mahjoubi S (2014) Infilled-pipe damper. J Constr Steel Res 98:45–58. https://doi.org/10.1016/j.jcsr.2014.02.015
83. Franco JM, Cahís X, Gracia L, López F (2010) Experimental testing of a new anti-seismic dissipator energy device based on the plasticity of metals. Eng Struct 32:2672–2682. https://doi.org/10.1016/j.engstruct.2010.04.037
84. Javanmardi A, Ghaedi K, Ibrahim Z, Muthu KU (2018) Seismic pounding mitigation of an existing cable-stayed bridge using metallic dampers. In: IABSE conference—engineering the developing world, International Association for Bridge and Structural Engineering, Kuala Lumpur, Malaysia, pp 617–623
85. Wang H, Zhou R, Zong ZH, Wang C, Li AQ (2012) Study on seismic response control of a single-tower self-anchored suspension bridge with elastic-plastic steel damper. Sci China Technol Sci 55:1496–1502. https://doi.org/10.1007/s11431-012-4826-5
86. Yamazaki S, Usami T, Nonaka T (2016) Developing a new hysteretic type seismic damper (BRRP) for steel bridges. Eng Struct 124:286–301. https://doi.org/10.1016/j.engstruct.2016.06.033
87. Ghaedi K, Ibrahim Z, Javanmardi A, Rupakhety R (2018) Experimental study of a new bar damper device for vibration control of structures subjected to earthquake loads. J Earthq Eng 00:1–19. https://doi.org/10.1080/13632469.2018.1515796
88. Ghaedi K, Ibrahim Z, Javanmardi A (2018, October). A new metallic bar damper device for seismic energy dissipation of civil structures. In: IOP Conference Series: Materials Science and Engineering. IOP Publishing, vol 431, No 12, p 122009
89. Motamedi M, Nateghi-A F (2018) Study on mechanical characteristics of accordion metallic damper. J Constr Steel Res 142:68–77. https://doi.org/10.1016/j.jcsr.2017.12.010
90. Aghlara R, Tahir MM (2018) A passive metallic damper with replaceable steel bar components for earthquake protection of structures. Eng Struct 159:185–197. https://doi.org/10.1016/j.engstruct.2017.12.049
91. Aghlara R, Tahir MM, Bin Adnan A (2018) Experimental study of Pipe-Fuse Damper for passive energy dissipation in structures. J Constr Steel Res 148:351–360. https://doi.org/10.1016/j.jcsr.2018.06.004
92. De Matteis G, Mazzolani FM, Panico S (2007) Pure aluminium shear panels as dissipative devices in moment-resisting steel frames. Int Assoc Earthq Eng 36:841–859. https://doi.org/10.1002/eqe
93. De Matteis G, Brando G, Mazzolani FM (2011) Hysteretic behaviour of bracing-type pure aluminium shear panels by experimental tests. Earthq Eng Struct Dyn 40:1143–1162. https://doi.org/10.1002/eqe
94. Rai DC, Annam PK, Pradhan T (2013) Seismic testing of steel braced frames with aluminum shear yielding dampers. Eng Struct 46:737–747. https://doi.org/10.1016/j.engstruct.2012.08.027

95. Robinson WH, Greenbank LR (1976) An extrusion energy absorber suitable for the protection of structures during an earthquake. Earthq Eng Struct Dyn 4:251–259. https://doi.org/10.1002/eqe.4290040306
96. Soydan C, Yuksel E, Irtem E (2014) The behavior of a steel connection equipped with the lead extrusion damper. Adv Struct Eng 17:25–39. https://doi.org/10.1260/1369-4332.17.1.25
97. Curadelli RO, Riera JD (2007) Design and testing of a lead damper for seismic applications. Proc Inst Mech Eng Part C J Mech Eng Sci 221(2007):159–164. https://doi.org/10.1243/0954406jmes254
98. Cheng S, Du S, Yan X, Guo Q, Xin Y (2017) Experimental study and numerical simulation of clapboard lead damper. Proc Inst Mech Eng Part C J Mech Eng Sci 231:1688–1698. https://doi.org/10.1177/0954406215621339
99. de la Llera JC, Esguerra C, Almazán JL (2004) Earthquake behavior of structures with copper energy dissipators. Earthq Eng Struct Dyn 33:329–358. https://doi.org/10.1002/eqe.354
100. Briones B, de la Llera JC (2014) Analysis, design and testing of an hourglass-shaped ETP-copper energy dissipation device. Eng Struct 79:309–321
101. Casciati F, Faravelli L, Petrini L (1998) Energy dissipation in shape memory alloy devices. Comput Civ Infrastruct Eng 13:433–442. https://doi.org/10.1111/0885-9507.00121
102. Sepúlveda J, Boroschek R, Herrera R, Moroni O, Sarrazin M (2008) Steel beam-column connection using copper-based shape memory alloy dampers. J Constr Steel Res 64:429–435. https://doi.org/10.1016/j.jcsr.2007.09.002
103. Zhang Y, Zhu S (2007) A shape memory alloy-based reusable hysteretic damper for seismic hazard mitigation. Smart Mater Struct 16:1603–1613. https://doi.org/10.1088/0964-1726/16/5/014
104. Dolce M, Cardone D, Marnetto R (2000) Implementation and testing of passive control devices based on shape memory alloys. Earthq Eng Struct Dyn 29:945–968. https://doi.org/10.1002/1096-9845(200007)29:7%3c945:AID-EQE958%3e3.0.CO;2-%23
105. Dolce M, Cardone D, Ponzo FC, Valente C (2005) Shaking table tests on reinforced concrete frames without and with passive control systems. Earthq Eng Struct Dyn 34:1687–1717. https://doi.org/10.1002/eqe.501
106. Ma H, Cho C (2008) Feasibility study on a superelastic SMA damper with re-centring capability. Mater Sci Eng, A 473:290–296. https://doi.org/10.1016/j.msea.2007.04.073
107. Ma H, Yam MCH (2011) Modelling of a self-centring damper and its application in structural control. J Constr Steel Res 67:656–666. https://doi.org/10.1016/j.jcsr.2010.11.014
108. Mata P, Barbat AH, Oller S, Boroschek R (2008) Constitutive and geometric nonlinear models for the seismic analysis of RC structures with energy dissipators. Arch Comput Methods Eng 15:489–539. https://doi.org/10.1007/s11831-008-9024-z
109. Ge H, Chen X, Matsui N (2011) Seismic demand on shear panel dampers installed in steel-framed bridge pier structures. J Earthq Eng 15:339–361. https://doi.org/10.1080/13632469.2010.491892
110. Kim DK, Dargush GF, Hu JW (2013) Cyclic damage model for E-shaped dampers in the seismic isolation system. J Mech Sci Technol 27:2275–2281. https://doi.org/10.1007/s12206-013-0610-0
111. A Javanmardi, Z Ibrahim, K Ghaedi, H Khatibi (2017) Numerical analysis of vertical pipe damper. In: 39th IABSE symposium engineering the future. International Association for Bridge and Structural Engineering, Vancouver, Canada, pp 2974–2980
112. Vasdravellis G, Karavasilis TL, Uy B, Asce M (2012) Design rules, experimental evaluation, and fracture models for high-strength and stainless-steel hourglass shape energy dissipation devices. J Struct Eng 140:04014087. https://doi.org/10.1061/(asce)st.1943-541x.0001014
113. Saffari H, Hedayat AA, Nejad MP (2013) Post-Northridge connections with slit dampers to enhance strength and ductility. J Constr Steel Res 80:138–152. https://doi.org/10.1016/j.jcsr.2012.09.023
114. Maleki S, Bagheri S (2010) Pipe damper, part II: application to bridges. J Constr Steel Res 66:1096–1106. https://doi.org/10.1016/j.jcsr.2010.03.011
115. Shen X, Camara A, Ye A (2015) Effects of seismic devices on transverse responses of piers in the Sutong Bridge. Earthq Eng Eng Vib 14:611–623. https://doi.org/10.1007/s11803-015-0049-7
116. Vasseghi A (2011) Energy dissipating shear key for precast concrete girder bridges. Sci Iran 18:296–303. https://doi.org/10.1016/j.scient.2011.05.036
117. Bayat M, Abdollahzadeh G (2011) Analysis of the steel braced frames equipped with ADAS devices under the far field records. Lat Am J Solids Struct 8:163–181. https://doi.org/10.1590/S1679-78252011000200004
118. Mahjoubi S, Maleki S (2014) Seismic performance assessment of steel frames equipped with a novel passive damper using a new damper performance index. Struct Control Heal Monit. https://doi.org/10.1002/stc
119. Kim J, Jeong J (2016) Seismic retrofit of asymmetric structures using steel plate slit dampers. J Constr Steel Res 120:232–244. https://doi.org/10.1016/j.jcsr.2016.02.001
120. Mahmoudi M, Abdi MG (2012) Evaluating response modification factors of TADAS frames. J Constr Steel Res 71:162–170. https://doi.org/10.1016/j.jcsr.2011.10.015
121. Chen Z, Dai Z, Huang Y, Bian G (2013) Numerical simulation of large deformation in shear panel dampers using smoothed particle hydrodynamics. Eng Struct 48:245–254. https://doi.org/10.1016/j.engstruct.2012.09.008
122. Benavent-Climent A, Mota-Páez S (2017) Earthquake retrofitting of R/C frames with soft first story using hysteretic dampers: energy-based design method and evaluation. Eng Struct 137:19–32. https://doi.org/10.1016/j.engstruct.2017.01.053
123. Mohammadi RK, Nasri A, Ghaffary A (2017) TADAS dampers in very large deformations. Int J Steel Struct 17:515–524. https://doi.org/10.1007/s13296-017-6011-y
124. Deng K, Pan P, Su Y, Xue Y (2015) Shape optimization of U-shaped damper for improving its bi-directional performance under cyclic loading. Eng Struct 93:27–35. https://doi.org/10.1016/j.engstruct.2015.03.006
125. Usami T, Lu Z, Ge H (2005) A seismic upgrading method for steel arch bridges using buckling-restrained braces. Earthq Eng Struct Dyn 34:471–496. https://doi.org/10.1002/eqe.442
126. Shen X, Wang X, Ye Q, Ye A (2017) Seismic performance of Transverse Steel Damper seismic system for long span bridges. Eng Struct 141:14–28. https://doi.org/10.1016/j.engstruct.2017.03.014
127. Li G, Jiang Y, Zhang S, Zeng Y, Li Q (2015) Seismic design or retrofit of buildings with metallic structural fuses by the damage-reduction spectrum. Earthq Eng Eng Vib 14:85–96. https://doi.org/10.1007/s11803-015-0008-3
128. Vargas R, Bruneau M (2007) Effect of supplemental viscous damping on the seismic response of structural systems with metallic dampers. J Struct Eng 133:1434–1444. https://doi.org/10.1061/(ASCE)0733-9445(2007)133:10(1434)
129. Vargas R, Bruneau M (2009) Experimental response of buildings designed with metallic structural fuses. II. J Struct Eng 135:394–403. https://doi.org/10.1061/(ASCE)0733-9445(2009)135:4(394)

130. Mazzolani FM (2008) Innovative metal systems for seismic upgrading of RC structures. J Constr Steel Res 64:882–895. https://doi.org/10.1016/j.jcsr.2007.12.017
131. Mazzolani FM, Della Corte G, D'Aniello M (2009) Experimental analysis of steel dissipative bracing systems for seismic upgrading. J Civ Eng Manag 15:7–19. https://doi.org/10.3846/1392-3730.2009.15.7-19
132. I Nuzzo, D Losanno, G Serino, LMB Rotondo (2014) A seismic-resistant precast R. C. system equipped with shear link dissipators for residential buildings. In: Second international conference in advance civil, structural and environmental engineering, vol 2, pp 249–254. https://doi.org/10.15224/978-1-63248-030-9-52
133. Tagawa H, Yamanishi T, Takaki A, Chan RWK (2016) Cyclic behavior of seesaw energy dissipation system with steel slit dampers. J Constr Steel Res 117:24–34. https://doi.org/10.1016/j.jcsr.2015.09.014